Supporting Information

Tuning Ligands Ratio Allows for Controlling Gold Nanocluster Conformation and Activating a Nonantimicrobial Thiol Fragrance for Effective Treatment of MRSA-induced Keratitis

Zeyang Pang[$], Ning Ren[$], Yujie Wu, Jie Qi, Fupin Hu, Yuan Guo, Yangzhouyun Xie, Dejian Zhou and Xingyu Jiang**

1. Experimental Methods:

Unless otherwise specified, all organic solvents, inorganic salts, and polymeric reagents were purchased from Sigma-Aldrich (https://www.sigmaaldrich.com/).

1. 1. Preparation of $Au_{25}(C5)_{18}$ and $Au_{23}(4MMP)_{16}$ GNCs

4-mercapto-4-methyl-2-pentanol (4MMP, >98%) was purchased from Alfa Aesar (https://www.fishersci.com/us/en/brands/I9C8LQ9O/alfa-aesar.html). The thiolated zwitterionic (C5) ligand was prepared according to a previous report in our group[1].

The $Au_{25}(C5)_{18}$ NC synthetic protocol was adopted from a previous report with a few modifications[2]. Briefly, chloroauric acid tetrahydrate (20 mM, 250 μL, Macklin Reagent, http://www.macklin.cn/) was mixed with C5 ligand solution (5 mM, 2 mL). The mixture became yellow with some turbidity, which turned clear upon adding NaOH (1 M, 100 μL), followed by 2 mL ethanol. Finally, 100 μL $NaBH_4$ (100 mM in 0.2 M NaOH) was added dropwise with vigorous stirring. The solution slowly changed from colorless to light brown. After 3 h, the product was purified with the 3 kDa cut-off Amicon® Ultrafiltration Units and washed thrice with deionized water (18.2 MΩ) until pH = 7.

The $Au_{23}(4MMP)_{16}$ NC was synthesized with a similar method by mixing chloroauric acid tetrahydrate (20 mM, 250 μL) with 4MMP ligand solution (final concentration 5 mM in 2 mL ethanol), accompanied by the formation of a pale-yellow solution. The subsequent addition of NaOH (13 μL, 1 M) turned the solution colorless. Subsequently, a mixture comprising 1 mL of ethanol and 1.7 mL of H_2O was introduced to maintain a final ethanol volume of ~60% (V/V). Finally, 100 μL $NaBH_4$ solution (100 mM in 0.2 M NaOH) was added dropwise with vigorous stirring, and the solution gradually turned yellowish-brown and finally to yellowish-green. The product was purified with 3 kDa cut-off Amicon® Ultrafiltration Units after a 3-h reaction and washed with 50% ethanol solution until the pH of the filtrate reached 7. After purification, the GNCs are sealed and aged in a dark environment at room temperature for over 24 h before use.

1. 2. Preparation of 4MMP-C5 dual-ligand-capped GNCs

For dual-ligand GNCs, the total concentration for the dual ligands feeding was kept unchanged (final concentration 5 mM in 2 mL ethanol, with only ligand feed ratios adjusted from 0−100%). The chloroauric acid tetrahydrate (20 mM, 250 μL) and the total volume of ethanol (~60% V/V) were fixed for GNCs with different ligand feed ratios. However, the amount of NaOH was adjusted according to the 4MMP ligand feed ratios. Specifically, the corresponding relationship is 10%−90 μL, 20%−83 μL, 30%−40 μL, and 40%−25 μL. When the feed ratios of the 4MMP ligand vary between 50% and 90%, the volume of NaOH remains constant at 13 μL. Taking GNC with 70% 4MMP in feed as an example, 1400 μL ethanol solution of 5 mM 4MMP was mixed well with 600 μL of 5 mM C5 before mixing with 20 mM, 250 μL chloroauric acid to acquire a pale-yellow solution. Then 13 μL of NaOH was pipetted to the solution and turned the solution colorless. Subsequently, 100 μL $NaBH_4$ solution (100 mM in 0.2 M NaOH) was added dropwise with vigorous stirring. After a 3-h reaction, the product was purified with 3 kDa cut-off Amicon® Ultrafiltration Units and washed with 50%

ethanol solution until the pH of the filtrate reached 7. After purification, the GNCs are sealed and aged in a dark environment at room temperature for over 24 h before use.

1. 3. Electrospray ionization-mass spectroscopy (ESI-MS) analysis of different GNCs

For ESI-MS analysis, the GNCs were diluted to a light brown solution with a final concentration of ~200 μg mL^{-1} and injected directly into the high-resolution mass spectrometry system (Q Exactive, Thermo Scientific, https://www.thermofisher.com/order/catalog/product/IQLAAEGAAPFALGMBDK) with a peristaltic pump. The data was further deconvoluted with *Thermo Scientific Protein Deconvolution* software with MH+ output mode. The Restricted Time, Chromatogram m/z Range, and Relative Intensity Threshold were adjusted according to the spectrum peak positions and the theoretical mass of the corresponding GNC species. The resolution was set to 50000, and the S/N threshold was 3. After mass deconvolution, the results were compared with the theoretical molecular weights of $Au_{25}(4MMP)_n(C5)_{18-n}$ or $Au_{23}(4MMP)_n(C5)_{16-n}$ GNCs with different 4MMP/C5 ratios in **Table S1** to designate the specific GNC species. The related results were summarized in **Table 1** in the main text.

1. 4. Transmission electron microscope (TEM) analysis of dual-ligand GNCs with different 4MMP ligand feed percentages

For TEM characterization of different GNCs, the stock solution of GNC was diluted >10,000 folds to a final concentration of ~0.1 μg mL^{-1} and pipetted 6 μL on the ultra-thin silicon nitride chips with a thickness of 15 nm (AR010A, YW.MEMS, https://www.topmems.com/en/). The chip was then dried overnight and observed with a Titan Themis G2 double spherical aberration-corrected transmission electron microscope (DSAC-TEM) under high-angle annular dark field (HAADF)-STEM mode (https://www.fei.com/). The sizes of different GNCs were statistically analyzed with *ImageJ*.

1. 5. Ultraviolet−visible (UV−vis) spectrophotometry analysis of GNCs

The stock solution of GNC was diluted to ~200 μg mL^{-1} and pipetted >2 mL to a quartz cuvette (As one, https://www.as-1.co.jp) to compare absorbance intensity with the reference solvent. The UV−vis spectrum was analyzed with a UV−vis spectrophotometer (PerkinElmer, Lambda 750s, https://www.perkinelmer.com/).

1. 6. Fluorescence spectrophotometry of GNCs with different 4MMP ligand feed ratios

The stock solution of GNC was diluted to ~200 μg mL^{-1} and pipetted 1 mL to a fluorescence cuvette (Agilent, https://www.agilent.com/). The cuvette was then sent to a fluorescence spectrometer (HORIBA, iHR320 equipped with an InGaAs detector, https://www.horiba.com/) with an 808 nm laser as the excitation.

The excitation spectrum was further measured with a steady-state/transient fluorescence spectrometer (Edinburgh Instruments, FLS980, https://www.edinst.com/products/fls-980-fluorescence-spectrometer/) with deionized water as the reference.

1. 7. NMR analysis of the product ligand ratio after GNC digestion

To analyze the ligand ratios on the surface of the produced GNCs with different ligand feed percentages, we digested the gold kernel of GNCs with I_2 and applied NMR to characterize the corresponding characteristic peaks for each ligand. Specifically, 5 mg of lyophilized GNC powder was mixed with 0.5 mL of deuterated methanol, then 5 mg I_2 was added to react with the gold kernel. The transition of the solution's color from brown to yellow, accompanied by the cessation of further change, signified the complete degradation of the gold core. We then vortexed the solution well and separated the supernatant for NMR analysis. The peak ratios at 1.19–1.39 ppm (9H) and ~2.88 ppm (6H, or 3.04–3.28 ppm, 6H) were used to determine the content of 4MMP and C5 ligands. The NMR spectra were provided with an AVANCE III 400M with the prodigy platform (BRUKER, https://www.bruker.com/en.html) and analyzed with *MestReNova*.

1.8. X-ray photoelectron spectroscopy (XPS) spectrometry of GNCs with 0% and 100% 4MMP ligand feed ratios

The GNC solution was lyophilized to dry powder in advance, then ~20 mg of the GNC powder was placed on the tinfoil paper. We folded the foil over the sample, pre-compacted it with glass slides, and finally compressed it with a tablet press. When the pressure indicator of the tablet press was 0.1 MPa, the sample was taken out for degaussing and then pasted on the sample stage with a 5 mm electrically conductive double-sided tape (NISSHIN, 7311, https://www.nisshin-em.co.jp/). After the height of the sample stage was adjusted, it was sent to an X-ray photoelectron spectrometer (K-Alpha, Thermo Scientific) with a monochromatic Al Kα X-ray source. When the pressure in the sample chamber was less than 2.0×10^{-7} mbar, the sample was sent into the analysis chamber. We applied a 400 μm spot size, and the working voltage was 12 kV. The filament current was 6 mA. The energy for the full-spectrum scanning was 150 eV with a step size of 1 eV, and the narrow-spectrum scanning energy was 50 eV with a step size of 0.1 eV. The obtained spectra were processed using *Avantage* software.

1. 9. Antibacterial effect analysis of GNCs with different 4MMP ligand feed percentages

For analyzing the minimum inhibitory concentration (MIC), pre-selected single colonies of different bacteria strains [*Staphylococcus aureus* (ATCC, 29213), *Staphylococcus epidermidis* (12228), *Staphylococcus hemolyticus* (29970), *Enterococcus faecalis* (29212), *Escherichia coli* (25922), *Pseudomonas aeruginosa* (27853), and *Klebsiella pneumoniae* (27736). Corresponding MDR strains were acquired from clinical isolation from Huashan Hospital pathological samples] were incubated in a 37 °C shaker for 24 h in the lysogeny broth (LB) medium. Before experiments, 10 μL of each bacterial solution was inoculated into 1 mL LB medium, and the solution was incubated for 6 h until the OD_{600} reached ~0.3. The broth-dilution method was employed to ascertain the MIC values for each bacterial strain. Briefly, to a 96 well-plate, 100 μL of LB medium was added to each well, followed by adding 100 μL of GNC

stock solution (or corresponding antibiotics) to the starting well. Upon thorough mixing, a 100 μL aliquot of the solution was extracted from the first well and transferred to the second well. This process was repeated until the penultimate well of the row. The last well was left for blank control, and every three rows were used as one replicate. Subsequently, the bacterial solution was diluted 1000 times and inoculated 10 μL into each well. The 96-well plate was then incubated under 37 °C for 16 h, and the lowest GNC concentration corresponding to no turbidity was defined as MIC. For the minimum bactericidal concentration (MBC) value, the incubation time was prolonged to over 24 h.

1. 10. Analysis of the hemolysis rates of dual-ligand GNCs with different 4MMP feed percentages

The hemolytic analysis was conducted by amalgamating GNCs of varying concentrations with a 2% suspension of red blood cells in equivalent proportions. The suspension was obtained by thrice washing whole murine blood with phosphate buffer saline (PBS) and subsequently combining 200 μL of hematocrit with 9.8 mL of PBS solution. 400 μL of the red blood cell suspension was then transferred to a 1.5 mL Eppendorf tube and mixed with the same volume of GNC solution with different concentrations. Deionized water was applied as the positive control, and the PBS solution was applied as the negative control. The samples were then incubated in a 37 °C water bath for 3 h, followed by a centrifuge (1500 rpm, 10 min) to take the supernatant for OD_{540} (A_{540}) measurement in a 96-well plate. The hemolytic rate was analyzed by the following formula:

$$\mathrm{HL} = \frac{A_{sample} - A_{negative}}{A_{positive} - A_{negative}} \times 100\% \quad (1)$$

Typically, a 5% hemolytic rate, denoted as HD_5, was applied to determine the hematological safety of each material.

1. 11. Molecular dynamic (MD) simulation

MD simulations were conducted between DPPG/DP3adLPG bilayer (DPPG: DP3adLPG = 7:3)[3] with $[Au_{23}(4MMP)_{16}]^-$ or $[Au_{23}(4MMP)_{14}(C5)_2]^-$ by *GROMACS 2021.5* package[4]. DPPG was parameterized by the Lipid17 force field, DP3adLPG's force field parameters and partial charges were modified from DPPG, the lysine part was derived from the general AMBER force field 2(GAFF2)[5], and the restrained electrostatic potential (RESP) charge. The structure and AMBER-compatible force field parameters of $Au_{23}(SR)_{16}$ NC were built as references[6]. Partial charges of both ligands (4MMP and C5) were optimized according to the suggestions in the literature[7]. *Ambertools21* and *ACPYPE* were used to construct the GAFF2 parameters[8], and *Multiwfn* was used to fit the RESP charge[9].

The initial structure of the lipid bilayer containing 202 DPPG and 46 DP3adLPG molecules was constructed by the genmixmem program (Tian Lu, http://sobereva.com/245, accessed: December 2022). 8.2 × 8.2 × 12.8 nm^3 cubic boxes with pre-equilibrated bilayers were established, and GNCs protected by different ligands ($[Au_{23}(4MMP)_{16}]^-$ or $[Au_{23}(4MMP)_{14}(C5)_2]^-$) were placed 1.4 nm away from the bilayers. These systems were then dissolved in TIP3P water, followed by adding 195 Na^+ and 78 Cl^- to maintain electrical neutrality. Energy minimization was performed using the steepest descent algorithm with a force tolerance of 500 kJ mol^{-1} nm^{-1}. In all three directions, periodic boundary conditions were imposed. Then these systems were relaxed for 1 ns under isothermal−isobaric ensemble (NPT) MD simulations, and position restraints with a constant of 1000 kJ mol^{-1} nm^{-2} in three directions were performed on heavy atoms of lipid and GNCs.

After completing the above steps, 200 ns NPT MD simulations were performed on two systems. The pressure was maintained at 1 bar by the Parrinello-Rahman barostat in a semi-isotropic manner (x-, y-, and z-directions), and the temperature was maintained at 310 K by the V-rescale thermostat[10]. The LINCS algorithm was performed to constrain the bond lengths of hydrogen atoms. Lennard-Jones interactions were calculated within a cut-off of 1.2 nm, and

electrostatic interactions beyond 1.2 nm were treated with the particle-mesh Ewald (PME) method with a grid spacing of 0.16 nm. *UCSF ChimeraX* was used to visualize all results[11].

1. 12. NIR-II imaging of the 4MMP-GNCs and MRSA bacterial solution after co-incubation

The NIR-II fluorescence images of dual ligand GNCs, as well as MRSA cells, were photographed with a NIR-II fluorescence animal imager (NIROPTICS, Series III 900/1700, equipped with an 808-nm laser source, http://www.nir-optics.com/). The machine parameters were configured to a laser power of 5 W (corresponding to a laser density of ~20 mW cm^{-2}), and a long-pass filter with a cutoff wavelength of 1020 nm was employed. For imaging the original mixture of MRSA cells with GNCs of different 4MMP ligand feed ratios before and after thrice washing with PBS, the incubation time was controlled to 6 h, and the exposure time was set to 2/200 ms. Fluorescence retention was subsequently computed as the fluorescence intensity ratio before and after washing, with exposure time standardized.

For the NIR-II fluorescence microscopic imaging, the MRSA cell solution (OD_{600} = 0.5) was incubated with 32 μg mL^{-1} 4MMP-GNCs for 8 h, washed 3 times, and redispersed in PBS solution. The bacterial smear was slightly dried on a coverslip and observed with a NIR-II microscopy imaging system (NIROPTICS, MicroVis−1000) with 3 W laser power and 100 ms exposure time.

1. 13. Inductively coupled plasma mass spectrometry (ICP-MS) analysis of the Au element content in the solution

To analyze the Au element content within the 4MMP-GNC solution, a 10 μL aliquot of the original GNC solution was extracted and combined with an equivalent volume of fresh aqua regia for digestion. The solution color suddenly changed to colorless, and the volume was diluted to 5 mL with 2% nitric acid solution (the original solution was diluted 500 times). The

solution was then sent to the ICP-MS equipment (7700X, Agilent, https://www.agilent.com/), and the measured concentration was back-calculated to the initial concentration.

For measuring Au element content within MRSA cells after washing, the original solution was inoculated 200 μL into each MS glass vial and boiled with 400 μL fresh aqua regia until dryness. Then 400 μL fresh aqua regia was introduced again, and this procedure was repeated 4 times until organic matter was fully digested into the remaining water-soluble ash. 1 mL water was then introduced to each vial, and the vials were placed on a shaker to dissolve the remains fully. Finally, 500 μL solution was taken out and diluted to 4 mL before sending it to ICP-MS equipment (the original solution was diluted 40 times). Three replicate groups were set up for each set of data.

1. 14. Scanning electron microscope (SEM) analysis of MRSA morphology

The MRSA solution was pre-incubated overnight to $OD_{600} = 2$ and diluted 100-fold. Then the MRSA solution was aliquoted 500 μL into each 1.5 mL Eppendorf tube and treated with 0.1 M PBS (pH = 7.4, same below), 4 μg mL^{-1} (2× MIC) or 16 μg mL^{-1} (8× MIC) 4MMP-GNCs. After incubation for 6 h, the MRSA cells were washed thrice with PBS, 15 min each time, and centrifuged at 8500 rpm, 10 min each time at 4 °C. The pellet was re-dispersed with a 2.5% glutaraldehyde solution (Leagene Biotechnology, http://www.leagene.com/). After overnight fixation, samples were rinsed thrice with PBS and post-fixed with 1% osmic acid solution (Ted Pella, https://www.tedpella.com/) for 1–2 h, then rinsed with PBS thrice. 30%, 50%, 70%, 80%, 90%, and 95% ethanol solutions in different levels were used for the gradient dehydration. For each level, samples were first equilibrated for 15 min (to avoid sample deformation or breakage) and repeated centrifugation to remove the supernatant. The pellet was redispersed in the ethanol solution of the next level. Finally, the sample was redispersed in fresh absolute ethanol and balanced for 20 min, dripped 10 μL on a clean silicon wafer surface, and dried in a critical point dryer (Quorom k850, Quorum Technologies,

https://www.quorumtech.com/) before imaging. The silicon wafer was then pasted on the sample stage with conductive tape. An ion sputter coater (Hitachi MC1000, https://www.hitachi-hightech.com/) was used to sputter Pt on samples for about 120 s before sending them into the SEM machine (Hitachi Regulus 8100). The voltage was set to 5 kV, and the images were acquired at 30k magnification.

1. 15. TEM sample preparation, morphological observation, and STEM-energy dispersive spectroscopy (EDS) mapping procedures of MRSA cells

For TEM imaging, the MRSA solution was pre-incubated overnight to $OD_{600} = 2$ and diluted 100-fold. Then the MRSA solution was aliquoted 500 μL into each 1.5 mL Eppendorf tube and treated with 0.1 M PBS (pH = 7.4, same below) or 16 μg mL^{-1} (8× MIC) 4MMP-GNCs. After incubation for 6 h, the MRSA cells were washed thrice with PBS, 15 min each time, and centrifuged at 8500 rpm, 10 min each time at 4 °C. The pellet was then fixed with 2.5% glutaraldehyde solution (Leagene Biotechnology) overnight at 4 °C, then rinsed with 0.1 M 4 °C PBS buffer thrice, 15 min each. After removing the supernatant, the bacterial pellet was wrapped inside an agarose gel. Then the sample was gradiently dehydrated with a series of 4 °C acetone solutions (including 30%, 50%, 70%, 80%, 90%, and 95%, every 15 min) and 100% acetone for 20 min each. The sample was incubated with a mixture of embedding agent and acetone (V/V = 1/3) for 1 h; then V/V = 1/1 for 3 h; finally, the pure-embedding agent was added, and the sample was incubated under a constant 37 °C overnight. After the initial osmotic embedding was completed, the pure embedding agent containing the sample was poured into the embedding plate, and the sample was inserted into the embedding plate and then baked in an oven at 60 °C for 48 h for polymerization. After the polymerization, the resin block was removed for ultrathin sections. The sample was sliced on the LEICA EM UC7 ultra-thin microtome (https://www.leica-microsystems.com/) to obtain 70−90 nm slices. After drying, the slices were caught with a copper mesh (EMCN, http://www.emcn.com.cn/) and suspended

in ultrapure water for 5 min, then stained in 2% uranyl acetate saturated alcohol solution for 8 min in the dark (for negative staining to provide contrast) and washed with 70% alcohol and ultrapure water each thrice. The copper mesh was dried and observed with HITACHI HT7700 TEM.

For EDS mapping, the negative staining step in sample pretreatment was avoided during sample preparation to prevent element interference. EDS mapping was performed with the STEM-HAADF mode of Talos F200X G2 (FEI).

1. 16. Analysis of membrane fluidity with laurdan

The membrane fluidity was probed with a membrane fluidity-sensitive dye—laurdan (Invitrogen, https://www.thermofisher.com/). Specifically, the MRSA cells were cultured within LB (Solarbio, https://www.solarbio.com/) with 0.2% glucose (Macklin) until the OD_{600} reached ~0.35. The bacteria were then washed with PBS thrice and incubated with 10 μM laurdan (dissolved within 1% V/V, DMF solution) for 5 min to facilitate the staining of the bacteria membrane. Then the MRSA cells were washed again with 0.2% glucose. Subsequent to aliquoting the MRSA solution, various antibiotics and GNCs were introduced and incubated for a duration of 6 h. The confocal images were taken with a laser scanning confocal microscope (Nikon Confocal A1R, https://www.healthcare.nikon.com/en/lifescience/index.html) with 405 nm laser excitation, and the fluorescence intensities at 460 and 500 nm were recorded. The general polarization (GP) level was calculated with the following equation:

$$\mathrm{GP} = \frac{I_{460} - I_{500}}{I_{460} + I_{500}} \quad (2)$$

1. 17. DilC12(3) membrane clusterization study

The membrane clusterization was analyzed with a membrane mimicking dye DilC12(3) (Enzo Life Sciences), which binds with the fluid phase regions on the cell membrane. We first cultured the MRSA cells overnight and diluted the bacteria solution 200-folds with LB

containing 2 μg mL^{-1} DilC12(3), 1.25 mM $CaCl_2$, and 1% (V/V) DMSO. The bacterial solution was subsequently cultured until an OD_{600} of ~0.3 was attained. After that, it was washed 4 times with PBS. The MRSA cells were then resuspended with the same solution and treated with either 4MMP-GNCs or antibiotics for 6 h. The fluorescence image was taken under 550 nm excitation and 564 nm emission.

1. 18. Measurement of potassium ion (K^+) change of MRSA after different treatments

The K^+ level of MRSA cells in different groups was analyzed by measuring the potassium-dependent pyruvate kinase function. Briefly, the phosphoenolpyruvate was converted to pyruvate by pyruvate kinase, which is positively correlated with K^+ concentration. Subsequently, the produced pyruvate reacted with reduced nicotinamide adenine dinucleotide (NADH) and transformed to lactate and oxidized nicotinamide adenine dinucleotide (NAD), accompanied by a significant peak intensity change at 340 nm. The K^+ level was measured with the bacterial K^+ concentration biological enzyme colorimetric quantitative detection kit (GENMED, GMS70032.9, http://www.sh-genmed.com/) following the instructions included.

1. 19. Membrane potential staining with MycoStain It™ Green and DiSC3(5)

The membrane potential intensity could be analyzed using an array of polarization-sensitive dyes. Here we applied two types of membrane potential dyes. MycoStain It™ Green (AAT Bioquest, https://www.aatbio.com/) is a fluorescent sensor that exhibits green fluorescence upon binding with the MRSA bacterial membrane. The fluorescence would shift toward red emission at higher membrane potentials, and the red/green ratio is strongly related to the membrane potential density. The MRSA cells were cultured to around 1×10^6 CFU mL^{-1} and then washed thrice with PBS. Then the bacterial suspension was aliquoted 500 μL each into centrifugation tubes and treated with either GNC or antibiotics. Then 5 μL stock solution of MycoStain It™ Green (100×) was pipetted to each centrifugation tube and the solution was further incubated for half an hour before being observed with a confocal microscope. The

fluorescence was analyzed with 488 nm excitation and monitored at 510−530 nm for green and 600−660 nm for red. The ionophore membrane potential inhibitor—carbonyl cyanide-m-chlorophenylhydrazone (CCCP) was applied as the positive control and was diluted to 10 μM for the application.

As a common membrane staining dye, DiSC3(5) (AAT Bioquest) demonstrates a fluorescence increase that is in good accordance with the bacteria membrane depolarization. MRSA cells were incubated at 37 °C until the OD_{600} value reached 0.3, then were washed thrice with 2-[4-(2-hydroxyethyl)piperazin−1-yl] ethanesulfonic acid (HEPES) buffer and 5 mM glucose with 3000 g centrifugation for 10 min. The pellet was then resuspended in LB with 5 mM glucose, 100 mM KCl and DiSC3(5) with a 4 μM final concentration. The solution was kept under 37 °C for 4 min with strict protection from light. Then the MRSA cells were washed thrice and incubated with 4MMP-GNC (2 μg mL^{-1}) for 6 h, and daptomycin (2 μg mL^{-1}) was selected as the positive control. The fluorescence was monitored under 640 nm excitation and 685 nm emission.

1. 20. ATP level assay of GNCs compared with antibiotics

The differences in the ATP level of GNC and antibiotics-treated groups were analyzed with an ATP level kit (Nanjing Jiancheng Bioengineering Institute, A095−1−1, http://www.njjcbio.com/). The variation of the content of ATP within organisms is related to the energy metabolism change. Normally, the ATP level could reflect cell states and indicate cell apoptosis, necrosis, or poisoned states. The mechanism of this kit is using creatine kinase to catalyze adenosine triphosphate and creatine to generate phosphocreatine, which could be further detected by phosphomolybdic acid colorimetry. All the experiments were conducted according to the kit instruction.

1. 21. ATPase level analysis of GNC compared with antibiotics

The differences in the total ATPase activity of GNC-treated groups compared with antibiotics were analyzed with a total ATPase kit (A070−1) purchased from Nanjing Jiancheng Bioengineering Institute. The ATPase locates in the cell membrane structure of bacteria cells and is significant in material transportation, energy conversion, and information transmission. In addition, during abnormal conditions in the body, the activity of this enzyme will be affected. Thus, the function of this enzyme could indicate the organism's health state. To measure the activity of ATPase, ATP was introduced and reacted with the enzyme. The hydrolysis of ATP would produce inorganic phosphorus as a product, and the activity of ATPase could be analyzed by detecting the amount of free phosphorus with phosphomolybdic acid colorimetry.

1.22. Analysis of drug resistance growth toward commercial ophthalmic antibiotics

Our experimental method refers to existing reports with some modifications[12][13]. *S. aureus* (ATCC 29213) was selected for drug resistance development testing. We pre-selected and amplified monoclonal colonies before the experiment. Then for different antibiotics and 4MMP-GNC, we first measured the corresponding MIC value. Next, we inoculated the original bacterial solution with an OD_{600} value of 2 at the ratio of 1:100 into 1 mL of LB medium containing different antibiotics or 4MMP-GNC at subinhibitory concentrations of 0.25× and 0.5× MIC. Three parallel samples were carried out in each group, and the concentration at which turbidity first occurred shall prevail. After the OD_{600} value of the test tube with the lowest multiple MIC reaches 2, the bacterial solution was inoculated 1:100 into 1 mL culture medium with 0.5× MIC and 1× MIC of different antibiotics or 4MMP-GNC. The above steps were repeated once a day, and the multiplier of the antibacterial concentration was recorded.

1. 23. Cell viability measurement

Cell lines used in this study include human umbilical vein endothelial cells (HUVEC, ATCC, CRL−1730) and human retinal pigment epithelial cells (ARPE−19, ATCC, CRL-2302). For both cell lines, the cells were cultured at a 37 °C cell incubator with a 5% CO_2 supply and were

passaged every three days; ~30% were passaged into new 90 mm petri dishes after digestion. For HUVECs, the culture medium was Ham's F−12K medium with 10% (V/V) fetal bovine serum (FBS) and 1 ‰ (V/V) 30 mg mL^{-1} endothelial cell growth supplement (ECGS). For ARPE−19, the culture medium was replaced with Dulbecco's modified eagle medium (DMEM)/F12 with 10% (V/V) FBS.

The cell viability of different groups was measured using the 3-(4,5-dimethyl-2-thiazolyl)-2,5-diphenyltetrazolium bromide (MTT, Beyotime, https://www.beyotime.com/index.htm) method and characterized with cell live-dead staining kit (KEYGEN BIOTECH, KGAF001, http://m.keygentec.com.cn/). Specifically, the cells were preincubated 5×10^5 mL^{-1} overnight in a 96-well plate. Then the 4MMP-GNC (80/120 μg mL^{-1}, final concentration) was added to each well of the 96-well plate, and the plate was further incubated for 12/24 h. After that, the working solution containing MTT (5 mg mL^{-1}) was used to replace the original medium. 4 h later, the solution was absorbed by a thick stack of napkins, and purple sediment was dissolved in 150 μL DMSO. After thorough mixing, the plate was placed on a shaker for 10 min to dissolve the crystals fully. The absorbance at 570 nm was measured with a microplate reader (Synergy H1, BioTek, https://www.biotek.com/). Cell viability was ascertained by computing the ratio of absorbance relative to the PBS group.

For confocal laser microscope imaging, 90 μL of 2×10^4 cell suspension was transferred to a glass bottom petri dish (35 mm) and then further incubated for 12 h. 10 μL of the test material was added, and the cells were incubated for another 12/24 h. Then the cells were stained with an adequate concentration of Calcein-AM and propidium iodide (PI) (~50 μg mL^{-1}) for 30 min. The confocal fluorescence images were taken with the 488 nm laser excitation and collected 515 nm (for Calcein-AM)/617 nm (for PI) emitting images.

1. 24. Animal experiments

All animal experiments were approved by the Animal Research Committees of the South China Agricultural University (SYXK2020-C013) and conducted in strict compliance with the relevant laws and ethical requirements in the Guide for the Care and Use of Laboratory Animals of the National Institute of Health. The mice were purchased from Charles River and temporarily housed in a barrier facility in the animal center. Specifically, the temperature was controlled at 20 °C −26 °C. The relative humidity was between 40% and 70%. The airflow in the cages was controlled at 0.2 m s^{-1}, and the minimum static pressure difference was 10 Pa. The animals were fed once a day with water renewed.

1. 25. The *in vivo* safety study and analysis of liver and kidney toxicity

The biosafety test of 4MMP-GNC was performed BALBc mice (female, 6−8 weeks old, ~18 g, SPF grade). Before injection, mice were evenly grouped (n = 4), shaved, and fasted over 12 h. 6/12 mg kg^{-1} GNC (100/200 μL, ~1.1 mg mL^{-1}) solution was applied through tail vein injection. For the corneal biosafety analysis, 2 μL of 120 μg mL^{-1} 4MMP-GNC was dropped every 6 h on the unilateral cornea of mice. After 3 days of the administration, the individuals were anesthetized and sacrificed after blood sampling. While for the long-term ocular drug application test, the experimental period was extended to 21 days. The main organs of the mice were dissected and fixed in a 4% paraformaldehyde (Solarbio) solution to characterize the pathological changes. The corneas were separated and fixed with a FAS eyeball fixative solution (Servicebio, G1109).

For the biosafety tests, the mice's blood samples were separately collected into an anticoagulant tube (Solarbio) and a procoagulant tube with separation glue (BD Pharmingen, https://www.bdbiosciences.com/). The samples in procoagulant tubes were centrifuged at 5000 rpm, 4 °C, for 10 min until the serum and blood cells were completely separated. The serum was then collected and sent 300 μL to an automatic biochemical analyzer (MS-480, NBMEDICAL, https://en.nbmedicalsystem.com/) to analyze multiple liver and kidney

biochemical indicators. The anticoagulant whole blood samples were sent to an animal blood cell analyzer (DYMIND, DF-52Vet, http://www.dymind.com.cn/). All the data were processed with *Origin 2018*.

For the metabolism analysis of 4MMP-GNC, after injection with 6 mg kg^{-1} 4MMP-GNC into the tail vein on Day 0, then the mice were anesthetized daily and photographed in supine and prone positions using a NIR-II fluorescent animal imager (NIROPTICS, series III 900/1700). The parameter was set to (λ_{EX} = 808 nm, 32 mW cm^{-2}, 400 ms, 1020 long-pass filter). On Day 1 and Day 5, two groups of mice were sacrificed separately, and their main organs were collected, photographed, weighed, ground, and digested with fresh aqua regia under heat for 4 times, 1 h each. After full tissue digestion, 2% nitric acid solution was added and shaken to dissolve overnight, and the solution was diluted 25 times to 5 mL and sent to ICP-MS for quantitative detection of Au element.

For the extremely high concentration challenge, up to 110 mg kg^{-1} of 4MMP-GNC (~10 mg mL^{-1}, 200 μL) was administered through tail vein injection. The body weight was monitored daily and compared with the PBS control.

1. 26. Paraffin embedding

All the organic solvents used were purchased from Sinopharm (http://www.sinopharm.com/), except for the EDTA decalcification fluid purchased from Servicebio (G1105).

The fixed corneas or eyeball tissues were rinsed and placed into a dehydrating basket. After that, they were subjected to dehydration in gradient alcohol within a dehydrator. Details as follow: 75% alcohol (2 h); 85% alcohol (2 h); 90% alcohol (1.5 h); 95% alcohol (2 h); anhydrous ethanol I (2 h); anhydrous ethanol II (2 h); phenyl alcohol solution (40 min); xylene I (40 min); xylene II (40 min); 65 °C melted paraffin I (0.5 h); melted paraffin II (1 h); 65 °C melted paraffin III (2 h 45 min). The wax-soaked tissue was then embedded in the embedding

machine. The melted wax was put into the embedding frame first. Before the wax solidified, tissues were taken out of the dehydration box and put into the embedding frame according to the requirements of the embedding surface. Cooling at –20 °C freezing table, the wax block was removed from the embedding frame and trimmed after solidification. The trimmed paraffin was blocked on a paraffin microtome for preparing 4 μm-thick sections. Sections were spread and flattened on the spreader machine filled with 40 °C warm water. The glass slides were used to pick up the tissue sections. The glass slides were then sent to a 60 °C oven to remove the wax and stored at room temperature.

1. 27. H&E staining process

The paraffin sections were dewaxed 15 min thrice and treated with gradient alcohol (from high to low concentration 100%, 95%, 90%, 80%, 70%, every 2 min) for rehydration and put in hematoxylin dye solution for 5 min, then rinsed with running water, and put in 0.5% hydrochloric acid alcohol solution for differentiation for 5 s. The sample was then rinsed with running water again and put in 1% eosin dye solution for 3 min. After gradient dehydration again, xylene was added to transparent samples for 20−30 min. The slices were resin-mounted and scanned with a digital pathology scanner (Pannoramic MIDI, 3D HISTECH, https://www.3dhistech.com/).

1. 28. Gram staining process

All the organic solvents used are purchased from Sinopharm, and the Gram staining solution kit is purchased from Servicebio (G1105).

The sections were dewaxed in sequence in xylene I (20 min)-xylene II (20 min)-anhydrous ethanol I (5 min)-anhydrous ethanol II (5 min)-75% ethyl alcohol (5 min), then rinsed with running water to remove extra alcohol. Gram staining solution A was dropped on the sections to stain for 10−30 s, washed, and shaken to dry. Then Gram staining solution B was added for 1 min, washed, and shaken to dry, followed by taking the Gram staining solution C and rinsing

the tissue for differentiation until the flow-down liquid was colorless. The glass slide was then shaken to dry. The sections were then immersed in Gram staining solution D for 1 s, washed, microscopic examined, and baked to dry. The dried sections were placed into three jars of absolute ethanol to dehydrate in sequence for 1 s, 3 s, and 5 s. Then the sections were immersed into clean xylene for 5 min for transparency and mounted with neutral balsam. The slices were scanned with a digital pathology scanner (Pannoramic MIDI, 3D HISTECH).

1. 29. The *in vitro* porcine corneal infection model

The preparation of the porcine infection model followed the method of Ubani-Ukoma, et al.[12] The fresh pig eyes were purchased from the local slaughterhouse and instantly dissected after the execution. The eyeballs were preserved in a frozen state in a refrigerator at a temperature of –80 °C until surgery. We first used a hole puncher with an 8 mm diameter (TED PELLA, Rapid-Core) to create wounds deep into the porcine cornea stroma. The cornea was then separated from the eyeball with a thin scleral ring (for structural support) with conjunctival tissue, iris, and ciliary body completely removed. The corneas were then immersed in 10% povidone-iodine solution (ZHONGYIHE, http://www.wuxizhongyi.com/) for 30 min for quick sterilization and washed several times before subsequent treatments. In preparation for the agar cornea model, sterilized porcine corneas were positioned upside-down within a silicone mold of equivalent size and filled with a melted agar medium. After the agar was solidified, we turned over the agar-filled corneas and placed them within deep agar plates separately. MRSA solution (1×10^4 CFU mL^{-1}) was dropped 1 μL in the center of the circle wound, spread evenly, and infected for 12 h. Subsequently, GNC and vancomycin were applied to separate groups with 2.5 μL every 6 h, thrice total. The antibacterial effect was photographed at the end of the treatment. For plate coating, the corneas in each group were cut through the edge of the puncher and immersed in 7 mL PBS-T (PBS + 3‰ Tween) solution in 15 mL centrifugation tubes. The centrifugation tubes were vortexed 5 times each and shaken upside down 5 times. We then

diluted the stock solution to 1×10^4, 1×10^5, and 1×10^6-fold and evenly spread 100 μL on the new agar plates. The plates were further incubated for 24 h before colony counting. The picture of corneas under ambient light was recorded with a Lab imaging system (Bio-rad, ChemiDoc MP, https://www.bio-rad.com/).

1. 30. The *in vivo* corneal infection model

The *in vivo* corneal infection model was built with C57 mice (female, 6−8 weeks old, ~18 g, SPF grade). Before the animal experiments, the mice were anesthetized by peritoneally injecting 2.5% tribromoethanol (12–15 μL g^{-1} Wt), and 0.5% proparacaine eye drop was dropped at 5 μL on each eye of the mice to enhance local anesthesia. The mice were then distributed into 5 groups, with 5 individuals in each group. We first created 5 groups of W-shaped scratches that are deep into the stroma on the cornea of mice with a BD insulin syringe (BD Biosciences) and infected them with 2 μL MRSA solution (5×10^8 CFU mL^{-1}). After ~24 h, the keratitis model was built up with obvious opacity on the cornea of both eyes. Then different treatments were applied to diverse groups with a frequency of thrice per day at 6-hour intervals. Opacity size changes in mice were recorded daily with a stereo microscope (Nikon, SMZ18). After that, a clean swab was applied to sample the eye discharge and suddenly immersed in 1 mL PBS-T. The solution was then spread 200 μL on the agar plate for colony counting. On day 4, the mice were sacrificed by neck dislocation, and their eyeballs were taken out and fixed with FAS eyeball fixative solution (G1109). After 24-h fixation, the eyeballs were taken out for the H&E and Gram staining.

1. 31. Mouse visual acuity measurement

Optomotor response/reflex (OMR) assays were conducted with a virtual visual stimulation space established by four screens (Shanghai XinRuan Information Technology Co., Ltd, XR-OT101, http://www.softmaze.com/). A camera above the standing platform was applied for real-time monitoring. OptoTrack software was developed by Shanghai XinRuan Information

Technology Co., Ltd. This system could track the movement of the mouse head for a given visual stimulus in real time and automatically detect the OMR results. Prior to the experiments, mice belonging to different groups were marked with distinct symbols. Parameters were adjusted to optimal for the experimental subjects. Five different frequencies (unit: cyc/deg) were set in this experiment: 0.03, 0.05, 0.1, 0.2, and 0.3. During the experiments, gratings started to move and switched directions every 6 s. The grating stimulation time of each spatial frequency was 60 s. The stimulation interval (0−20 s) and the order of spatial frequency are randomly arranged for each mouse. Each group was measured 6 times. The movement of the mouse head was automatically recognized and detected by the analysis software. After each experiment, the platform was wiped and disinfected thoroughly to avoid inter-individual influences.

1. 32. Statistical analysis

Data were presented as the means ± standard deviation (SD). The *in vitro* experiments were performed in three independent experiments with at least three repetitions for each group. All statistical data analysis was determined by t-tests or one-way analysis of variance using *Excel* software. In this study, a *P*-value less than 0.05 was considered statically significant.

2. Figures and Tables

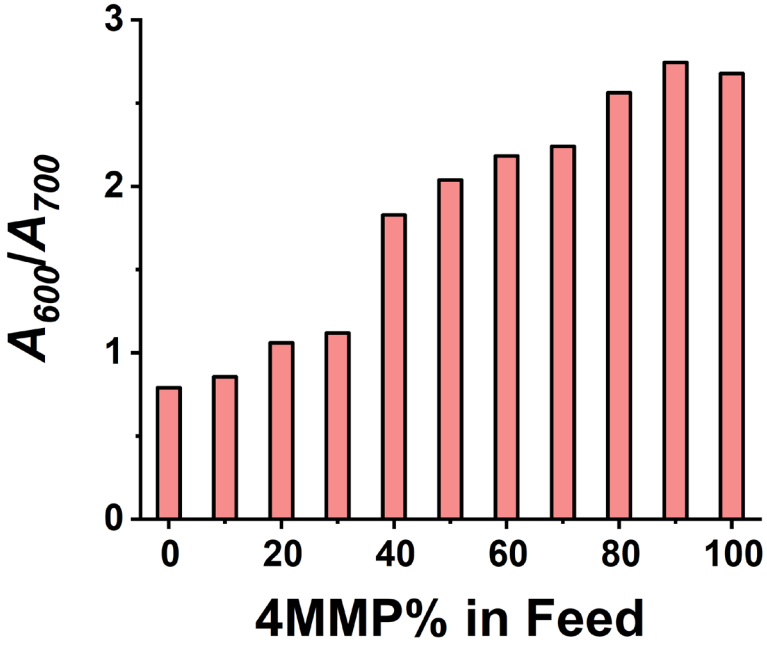

Figure S1. The plot of the absorbance ratio at 600 and 700 nm (A_{600}/A_{700}) *vs.* 4MMP ligand feed ratios. The curve has indicated the increase of the proportion of Au_{23} NC to Au_{25} NC with the 4MMP ligand percentage increasing.

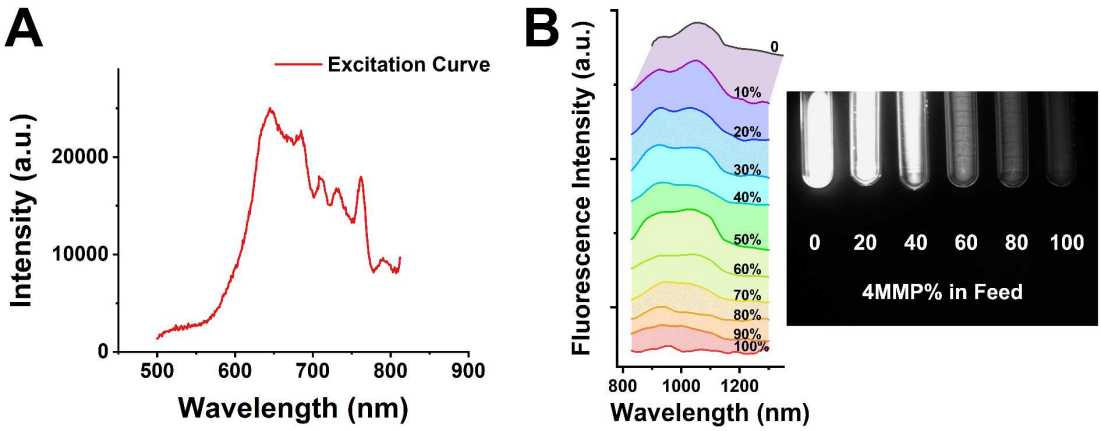

Figure S2. (A) NIR fluorescence excitation curve and (B) Photoluminescence spectra of 4MMP-C5 GNCs with different 4MMP feed ratios. The right inset in (B) shows the NIR fluorescence intensity of GNCs with different 4MMP feed percentages (from 0 to 100%, λ_{EX} = 808 nm with a 1020 nm long-pass filter, 60 ms). With the increase of the 4MMP ligand ratio as well as the proportion of $Au_{23}(SR)_{16}$ GNC in the product, the NIR fluorescence of dual ligand GNCs is gradually weakened, which is consistent with the photoluminescence spectra.

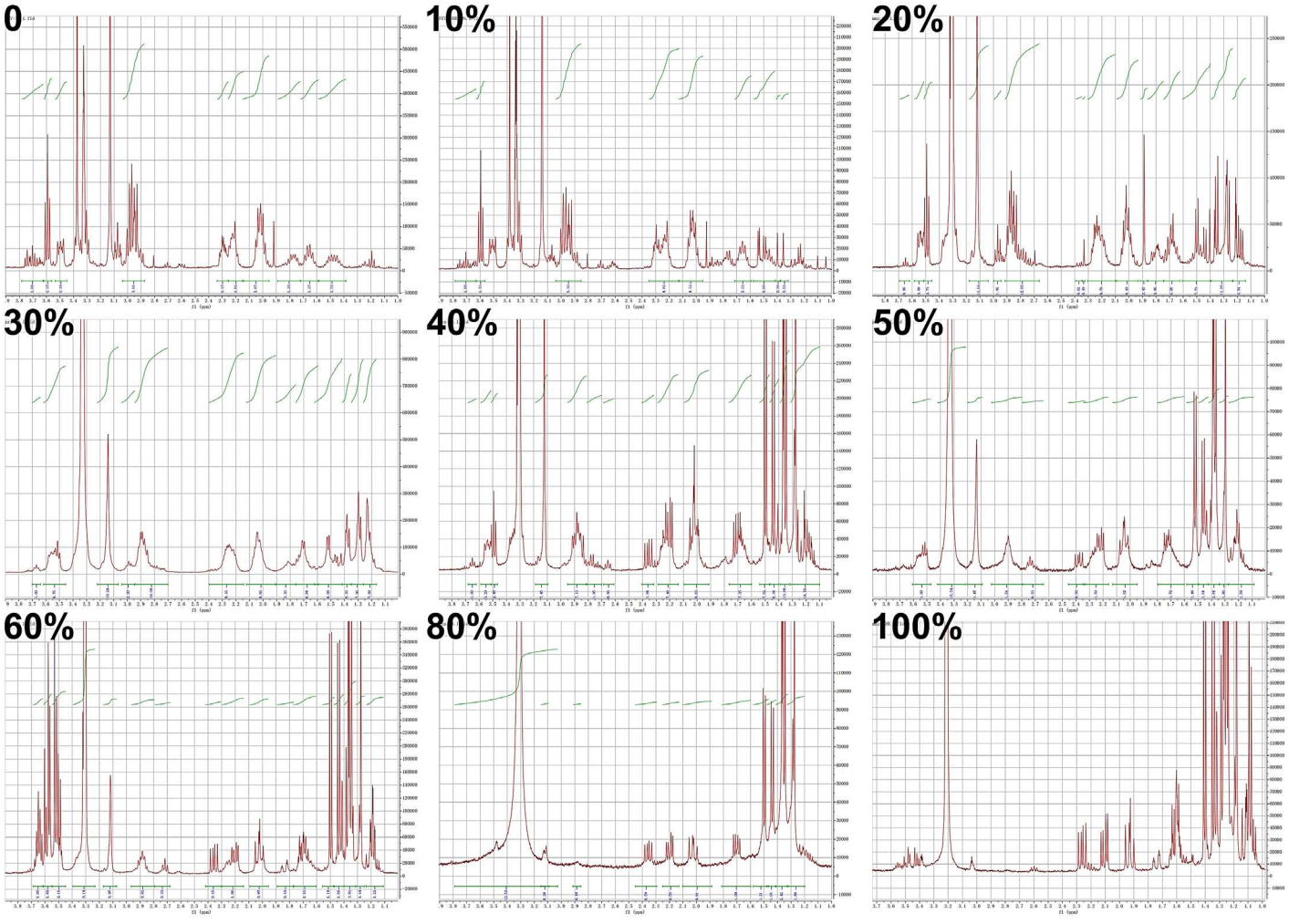

Figure S3. NMR spectra of GNCs with different 4MMP feed percentages after Au kernel digestion.

Table S1. Theoretical molecular weight of $Au_{25}(4MMP)_n(C5)_{18-n}$ or $Au_{23}(4MMP)_n(C5)_{16-n}$ prepared with different 4MMP/C5 ratios

$Au_{25}(4MMP)_n(C5)_{18-n}$ GNC structure	Corresponding GNC MW (Da)	$Au_{23}(4MMP)_n(C5)_{16-n}$ GNC structure	Corresponding GNC MW (Da)
$Au_{25}(4MMP)_{18}(C5)_0$	7323	$Au_{23}(4MMP)_{16}(C5)_0$	6663
$Au_{25}(4MMP)_{17}(C5)_1$	7543	$Au_{23}(4MMP)_{15}(C5)_1$	6883
$Au_{25}(4MMP)_{16}(C5)_2$	7763	$Au_{23}(4MMP)_{14}(C5)_2$	7103
$Au_{25}(4MMP)_{15}(C5)_3$	7983	$Au_{23}(4MMP)_{13}(C5)_3$	7323
$Au_{25}(4MMP)_{14}(C5)_4$	8203	$Au_{23}(4MMP)_{12}(C5)_4$	7543

$Au_{25}(4MMP)_{13}(C5)_5$	8423	$Au_{23}(4MMP)_{11}(C5)_5$	7762
$Au_{25}(4MMP)_{12}(C5)_6$	8643	$Au_{23}(4MMP)_{10}(C5)_6$	7982
$Au_{25}(4MMP)_{11}(C5)_7$	8863	$Au_{23}(4MMP)_9(C5)_7$	8202
$Au_{25}(4MMP)_{10}(C5)_8$	9083	$Au_{23}(4MMP)_8(C5)_8$	8422
$Au_{25}(4MMP)_9(C5)_9$	9303	$Au_{23}(4MMP)_7(C5)_9$	8642
$Au_{25}(4MMP)_8(C5)_{10}$	9523	$Au_{23}(4MMP)_6(C5)_{10}$	8862
$Au_{25}(4MMP)_7(C5)_{11}$	9742	$Au_{23}(4MMP)_5(C5)_{11}$	9082
$Au_{25}(4MMP)_6(C5)_{12}$	9962	$Au_{23}(4MMP)_4(C5)_{12}$	9302
$Au_{25}(4MMP)_5(C5)_{13}$	10182	$Au_{23}(4MMP)_3(C5)_{13}$	9522
$Au_{25}(4MMP)_4(C5)_{14}$	10402	$Au_{23}(4MMP)_2(C5)_{14}$	9742
$Au_{25}(4MMP)_3(C5)_{15}$	10622	$Au_{23}(4MMP)_1(C5)_{15}$	9962
$Au_{25}(4MMP)_2(C5)_{16}$	10842	$Au_{23}(4MMP)_0(C5)_{16}$	10182
$Au_{25}(4MMP)_1(C5)_{17}$	11062	–	–
$Au_{25}(4MMP)_0(C5)_{18}$	11282	–	–

0

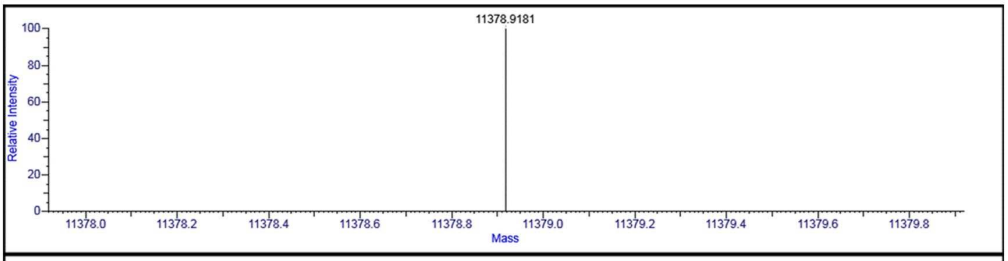

10%

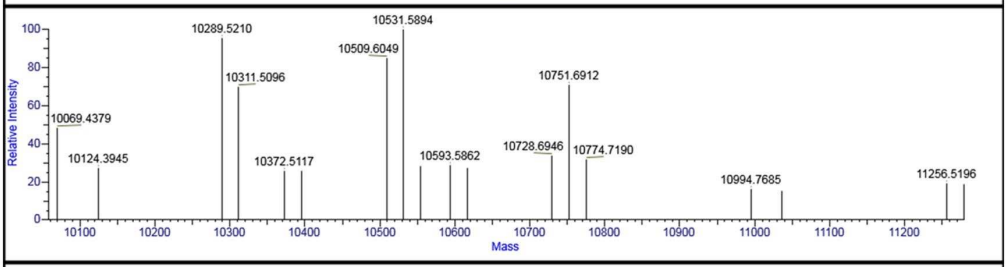

20%

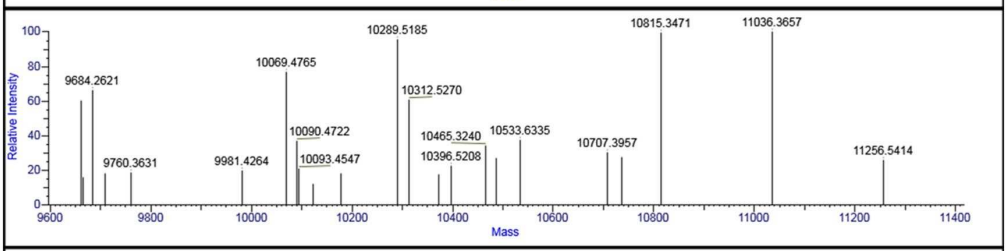

30%

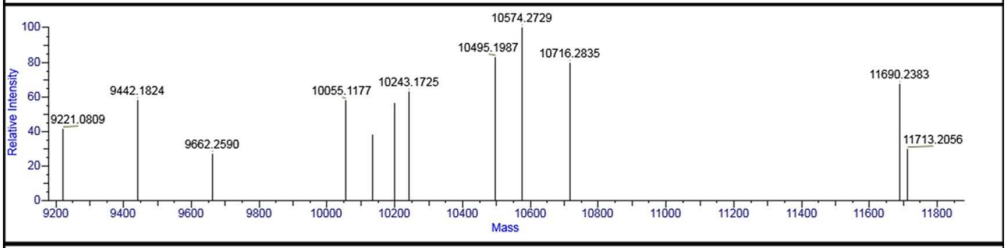

40%

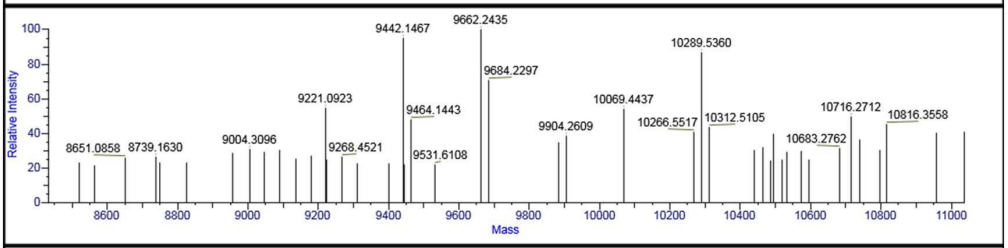

50%

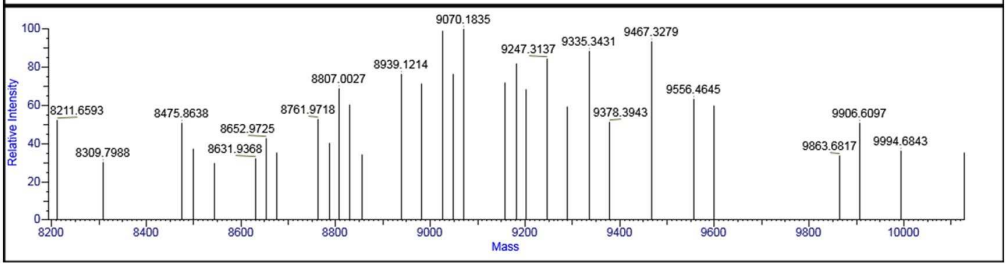

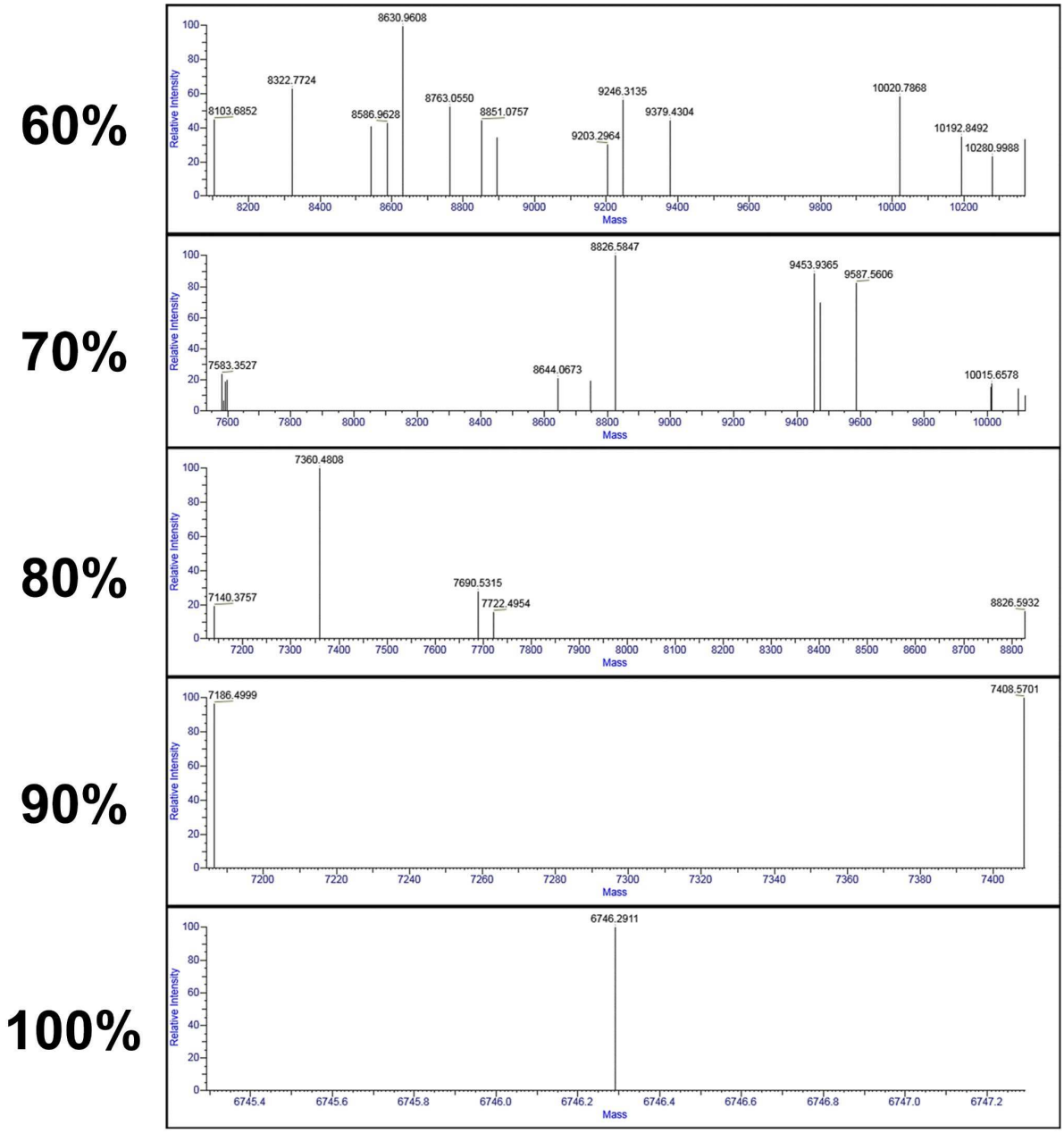

Figure S4. Deconvoluted results of the ESI-MS spectrum showing the overall molecular mass change from $Au_{25}(C5)_{18}$ to $Au_{23}(4MMP)_{16}$ with the increase of 4MMP ligand feed percentages, accompanied by the reduction of the molecular weight.

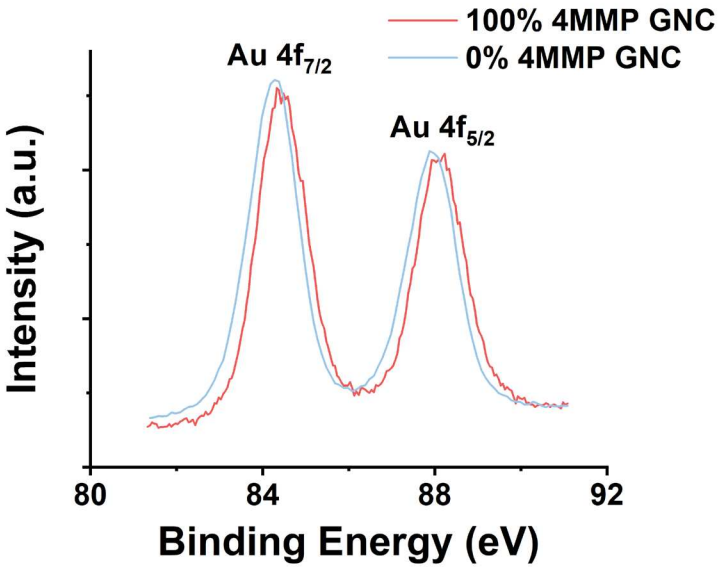

Figure S5. XPS spectra of the Au $4f_{7/2}$ and $4f_{5/2}$ orbitals of GNCs with 0 (blue line) and 100% (red line) 4MMP in feed.

Table S2. MIC values for each ligand and their mixture with the equivalent amount of Au ions required for the synthesis of 4MMP-C5 dual-ligand capped GNCs against a panel of selected bacterial species. (Unit: μg mL^{-1})

Ligand type	*S. a*	MRSA	*S.e*	MRSE	*S.h*	MDR *S.h*	*E.f*	VRE	*E.c*	*K.p*	*P.a*
4MMP	>2048	>2048	>2048	>2048	>2048	>2048	>2048	>2048	>2048	>2048	>2048
C5	>2048	>2048	>2048	>2048	>2048	>2048	>2048	>2048	>2048	>2048	>2048
4MMP + Au^{3+}	>2048	>2048	>2048	>2048	>2048	>2048	>2048	>2048	>2048	>2048	>2048
C5 + Au^{3+}	>2048	>2048	>2048	>2048	>2048	>2048	>2048	>2048	>2048	>2048	>2048
4MMP + C5 + Au^{3+}	>2048	>2048	>2048	>2048	>2048	>2048	>2048	>2048	>2048	>2048	>2048

Table S3. The MIC of GNCs prepared with different 4MMP feed ratios against MDR gram-positive strains (unit: μg mL^{-1})

4MMP feed (%)	MRSA	MRSE	MDR *S. h*	VRE
0	>256	>256	>256	>256
10	>256	>256	>256	>256
20	>256	>256	>256	>256
30	16	>256	>256	>256
40	8	256	32	128
50	4	32	16	128
60	4	16	16	32
70	2	4	8	4
80	2	4	8	4
90	2	4	8	8
100	16	16	16	32

Table S4. The MBC of GNCs prepared with different 4MMP feed ratios against MDR gram-positive strains (unit: μg mL^{-1})

4MMP feed (%)	MRSA	MRSE	MDR *S. h*	VRE
0	>256	>256	>256	>256
10	>256	>256	>256	>256
20	>256	>256	>256	>256
30	>256	>256	>256	>256
40	>256	>256	>256	>256
50	16	64	128	>256
60	16	64	64	64
70	8	16	32	16
80	8	16	32	16
90	4	16	64	8
100	32	128	128	128

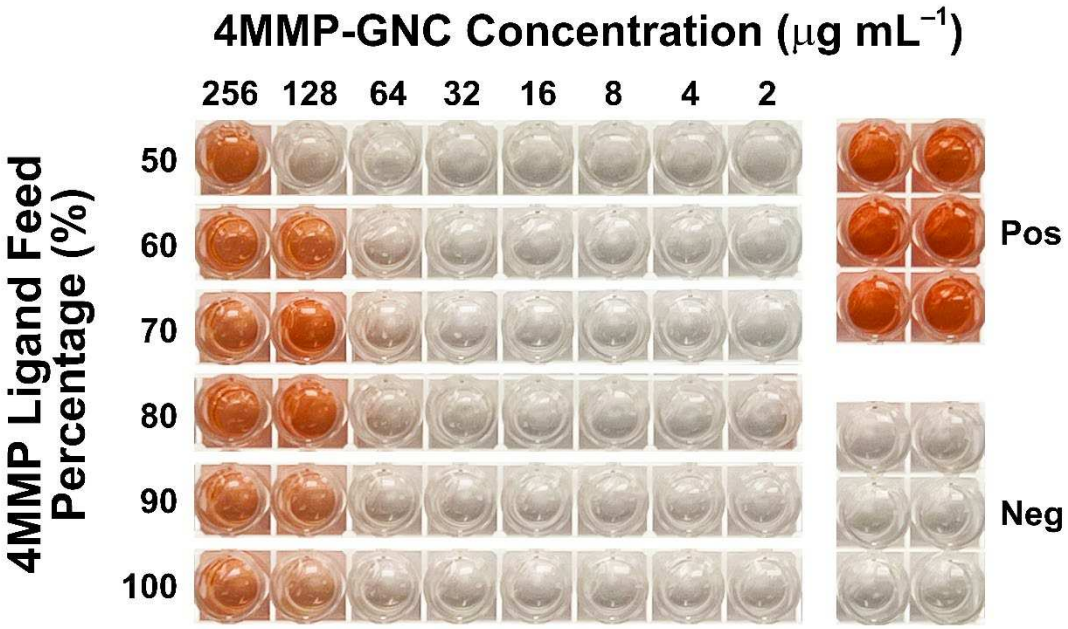

Figure S6. The ambient light picture of hemolytic data of 4MMP-GNC with 4MMP ligand feed percentages ranging from 50% to 100%. The data is linked to **Figure 2D** in the main text. Comparatively, the hemolytic activities of different GNCs are similar, with the GNCs with 4MMP ligand feed percentages of 70% and 80% demonstrating the highest hemolytic level.

Table S5. Comparison of the antibacterial spectrum and MIC values between 4MMP-GNC and other literature GNCs against gram-positive bacteria

Ligand Name	MICs[a] against gram-positive bacteria species[b]	Ref.
4MMP/C5	*S. a** (2 μg mL^{-1}), *S. e** (4 μg mL^{-1}), *S. h** (8 μg mL^{-1}), *E. f** (8 μg mL^{-1})	This study
4,6-Diamino-2-mercaptopyrimidine	*S. a** (5 μg mL^{-1}), *S. e** (5 μg mL^{-1}), *S. p** (5 μg mL^{-1}), *S. h** (5 μg mL^{-1})	[14]
Ampicillin/Lysozyme	*S. a** (>16 μg mL^{-1})	[15]
Bacitracin	*S. a* (200 μg mL^{-1})	[16]
Vancomycin	*S. a* (No Data)	[17]
Citraconyl moieties-decorated CysHHC10	*S. a* (16 μg mL^{-1}), *S. e* (4 μg mL^{-1})	[18]
NBC2253/NBC2254	*S. a** (3.0 ± 0.02 μM)	[19]
Mercaptoundecyl trimethyl quaternary ammonium	*B. s* (2.5 μg mL^{-1}), *E. f** (10 μg mL^{-1}), *S. a** (5 μg mL^{-1}), *S. e** (10 μg mL^{-1}), *S. h* (5 μg mL^{-1}), and *S. p* (2.5 μg mL^{-1})	[13]
(11-Mercaptoundecyl)-N, N, N trimethylammonium Bromide	*B. s* (3 μg mL^{-1}), *E. f** (1 μg mL^{-1}), and *S. p* (4 μg mL^{-1})	[20]

p-Mercaptobenzoic acid	*S. a* (~2.4 × 10^{15} particle mL^{-1} ≈ 4 μM)	[21]
p-Mercaptobenzoic acid	*S. a* (17.28 mM)	[22]
Mercaptohexanoic acid	*S. a* (2.5 μM), *S. e* (2.8 μM), and *B. s* (2.7 μM)	[23]
Mercaptohexanoic acid	*S. a* (>200 μM), and *B. s* (>200 μM)	[24]
Mercaptopyrimidines	*S. a** (2 μg mL^{-1}), and *E. f** (8 μg mL^{-1})	[25]
4,6-Diamino-2-mercaptopyrimidine	*S. a** (5 μg mL^{-1}), *S. e** (5 μg mL^{-1}), *E. f** (5 μg mL^{-1}), and *S.p** (5 μg mL^{-1})	[26]
Histidine	*B. s* (80 μM), *S. a** (80 μM)	[27]
1-Vinylimidazole	*S. a* (>35 μM)	[28]
Lysozyme	*S. a* (200 μM)	[29]
DNase	*S. a** (>128 μg mL^{-1}), and *S. e** (>128 μg mL^{-1})	[30]
Graphene oxide/ 6-Mercaptohexanoic acid/ Cysteamine	*S. a** (9.8 mg L^{-1})	[31]
4,6-Diamino-2-mercaptopyrimidine/Daptomycin	*S. a** (10 μg mL^{-1})	[32]
5-Methyl-2-thiouracil/ Protamine	*S. a** (0.011 mM)	[33]
Titanium Carbide (Mxene)/ *p*-mercaptobenzoic acid)	*S.a* (25 μg mL^{-1} + 0.085 μM)	[34]
Pyridinium/Zwitterionic ligands	*S. a** (8 μg mL^{-1}), and *S.e** (4 μg mL^{-1})	[1]
Cinnamaldehyde	*S. a** (30 μM)	[35]
Dodecyl trimethyl ammonium chloride	*S. a** (12.5 μg mL^{-1})	[36]
Mercaptohexanoic acid/ ZwBuEt	*S. a* (>25 μg [Au] mL^{-1})	[37]
Triphenylphosphine monosulfonate/ Tetraacetylated thioglucose	*S. a* (1.4 μg [Au] mL^{-1}), and *E. f* (1.4 μg [Au] mL^{-1})	[38]
Ac-YGRKKRRQRRR-(β-Ala)-(β-Ala)-(β-Ala)-Cys-$CONH_2$/ thiolated polyethylene glycol	*S. a* (>800 μg mL^{-1})	[39]
Thiolated D-maltose/Thiourea	*S. a* (0.25 μg mL^{-1} + 512 μg mL^{-1}), and *S. e* (0.125 μg mL^{-1} + 512 μg mL^{-1})	[40]
4,6-Diamino-2-mercaptopyrimidine	*B. s** (4 μg mL^{-1}), and *S. e** (4 μg mL^{-1})	[41]

[a)]MIC values are compared by the total mass of the antimicrobial material. Weaker antibacterial effects compared to this study are marked in red.

[b)]*B. s*—*Bacillus subtilis*, *S. a*—*Staphylococcus aureus*, *S. e*—*Staphylococcus epidermidis*, *S. h*—*Staphylococcus hemolyticus*, *S. p*—*Streptococcus pneumoniae*, and *E. f*—*Enterococcus faecalis.* Asterisk (*) indicates corresponding multidrug-resistant strains.

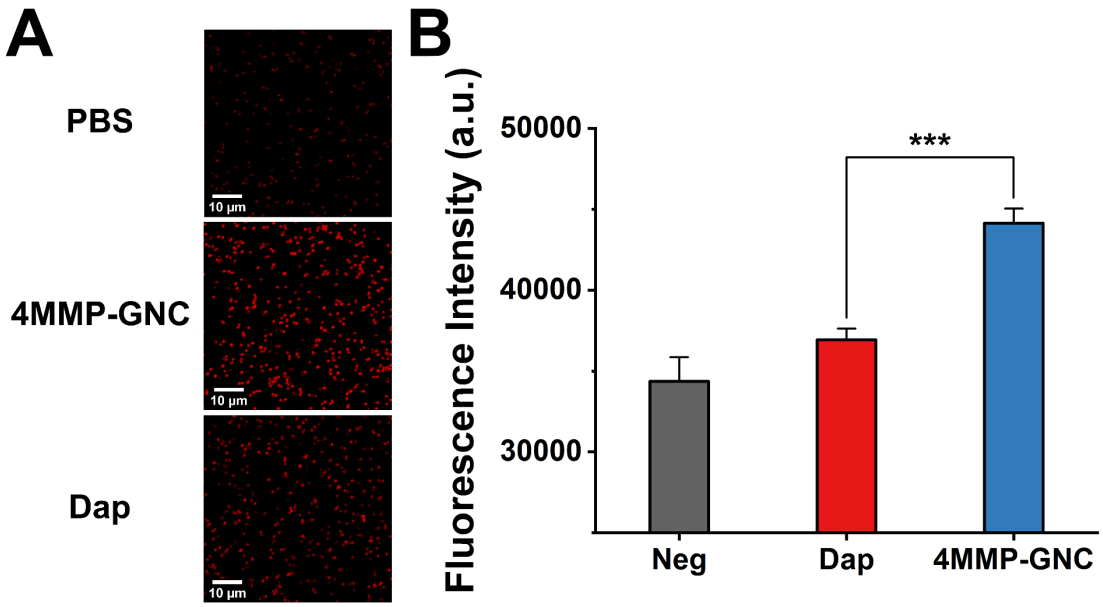

Figure S7. DiSC3(5) fluorescence images (left) and the corresponding statistical bar chart (right) of MRSA after 6-h incubation demonstrating the cell membrane potential dissipation induced by 2 μg mL^{-1} of Dap and 4MMP-GNC. (***: P <0.01)

Table S6. Influence of Ca^{2+} concentration on the antibacterial efficiency (MIC, μg mL^{-1}) of 4MMP-GNC and Dap.

Ca^{2+} concentration (mM)	4MMP-GNC	Dap
0	2	16
1.25	2	0.5

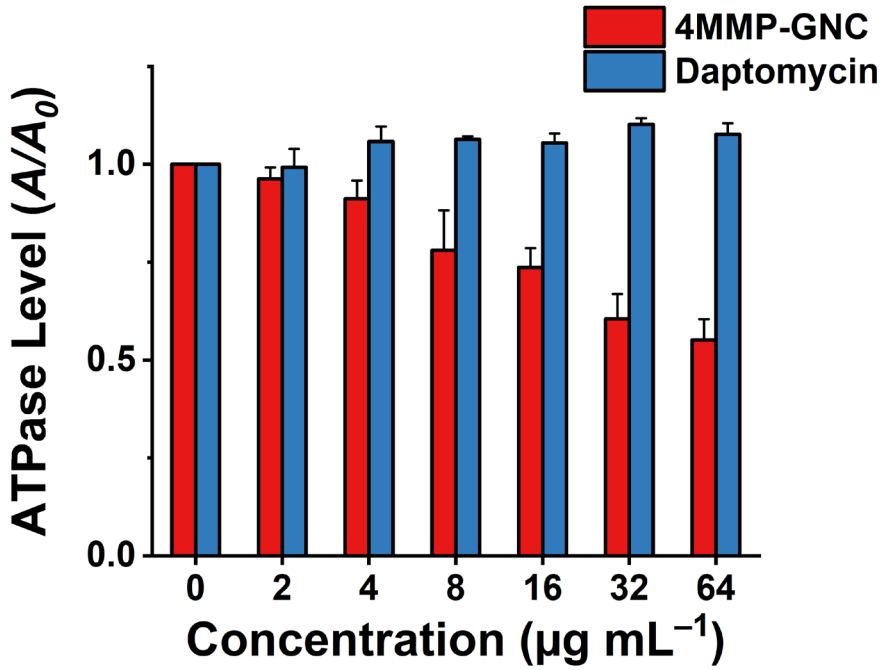

Figure S8. The ATPase activity of 4MMP-GNC- and Dap-treated MRSA cells at different doses.

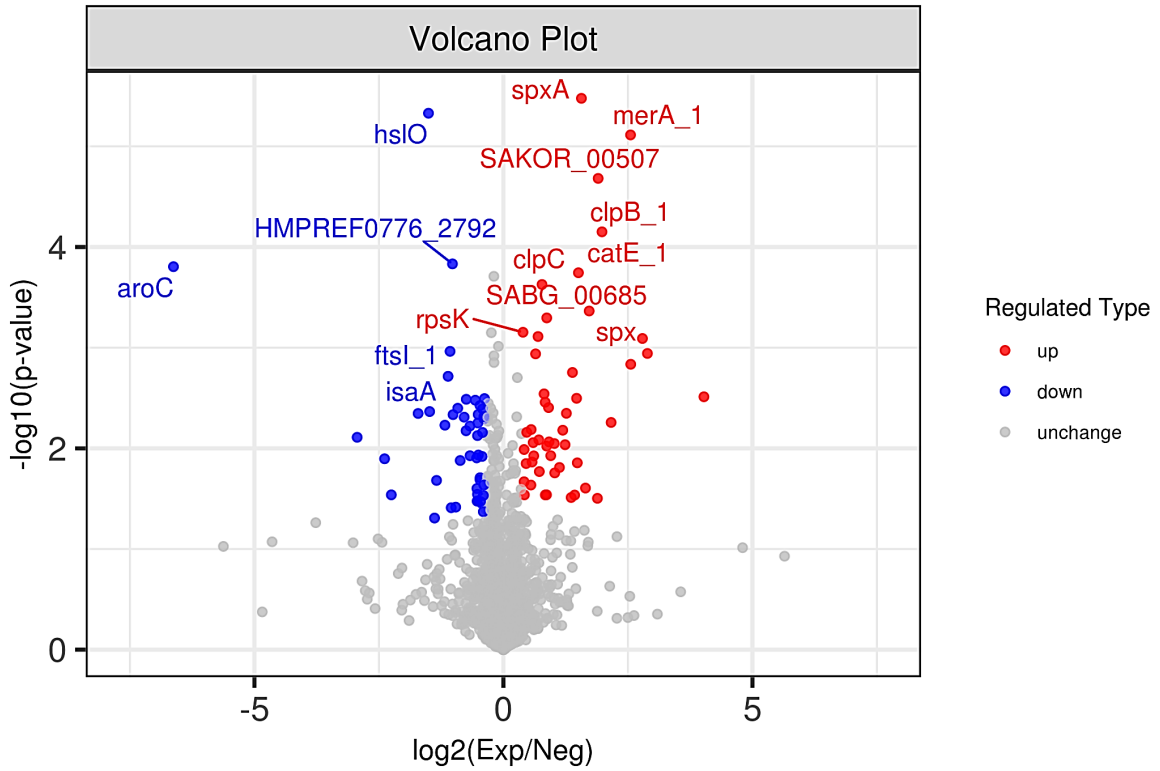

Figure S9. Volcano map of protein differential expression in the 4MMP-GNC group (Exp) compared to the control group (Neg). Fold change >1.3 and P <0.05 are significantly upregulated protein species marked in red. Fold change <0.77 and P <0.05 are significantly downregulated protein species marked in blue. Others are regarded as indistinct protein types and are marked in grey.

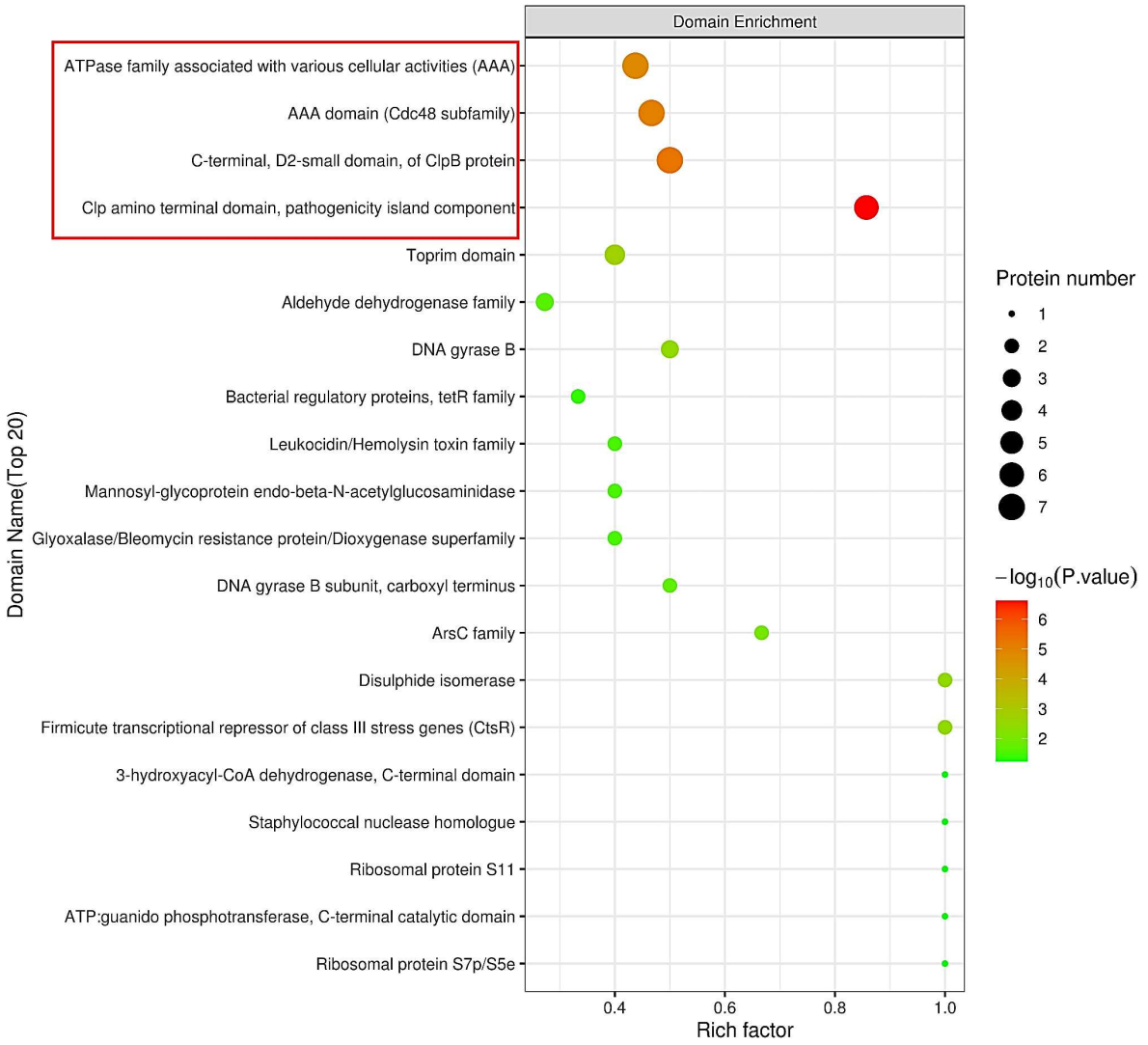

Figure S10. Domain enrichment analysis bubble chart between groups of the differentially expressed protein in MRSA with or without the treatment of 4MMP-GNC. The rich factor is the ratio of the number of differentially expressed proteins to the number of all annotated proteins in this pathway. The size of each bubble represents the number of differentially expressed proteins, with the redder the color, the more obvious the difference in expression, same below. Groups with high protein expression differences or quantities are marked within red boxes.

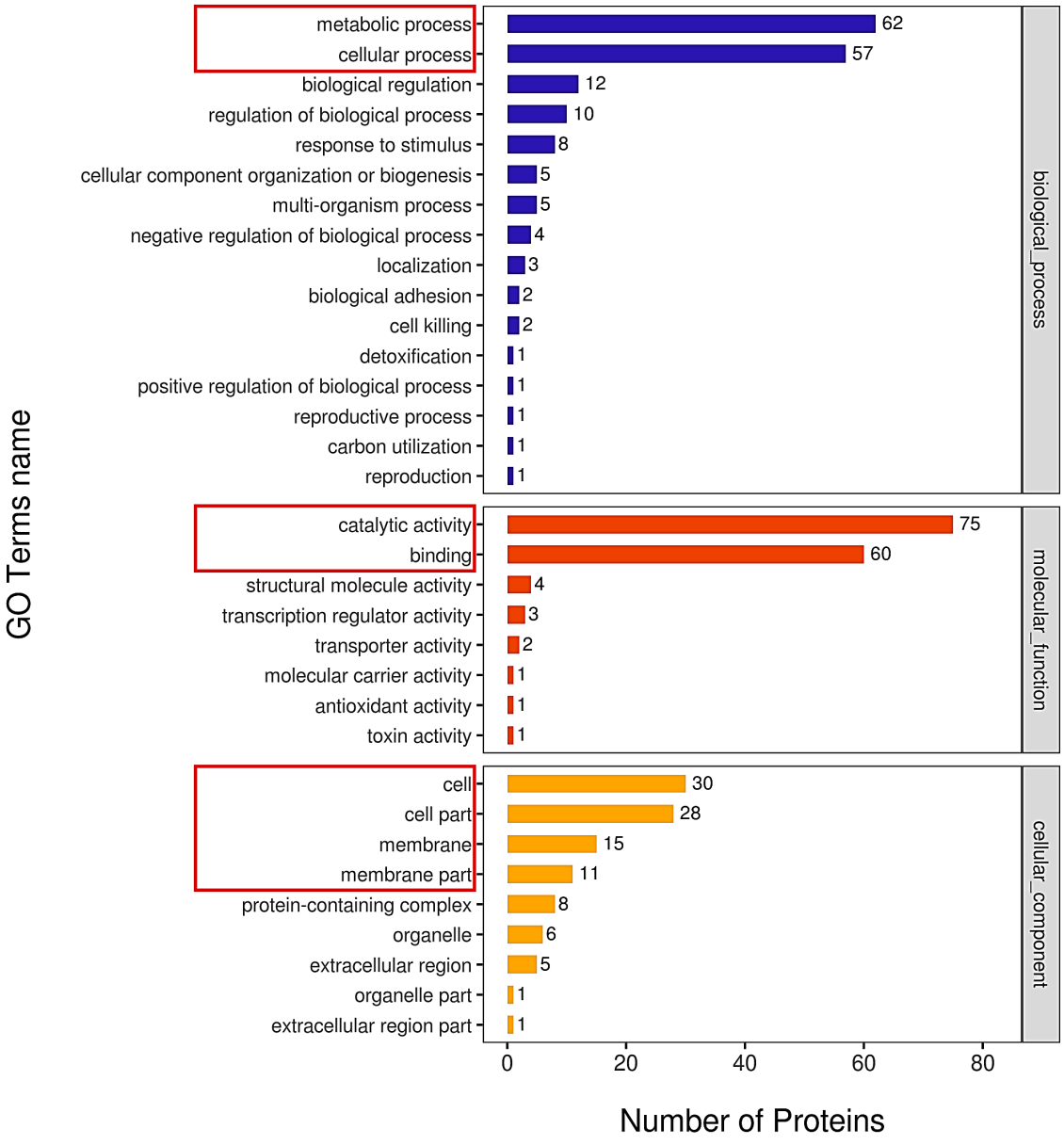

Figure S11. Gene ontology (GO) annotation statistics of differentially expressed proteins in the 4MMP group compared with the control group, arranged according to the number of differentially expressed proteins involved in each process. The y-axis is the secondary function annotation information (GO Level2), including **Biological Process**, **Molecular Function**, and **Cellular Component** three categories, arranged from top to bottom according to the number of differentially expressed proteins.

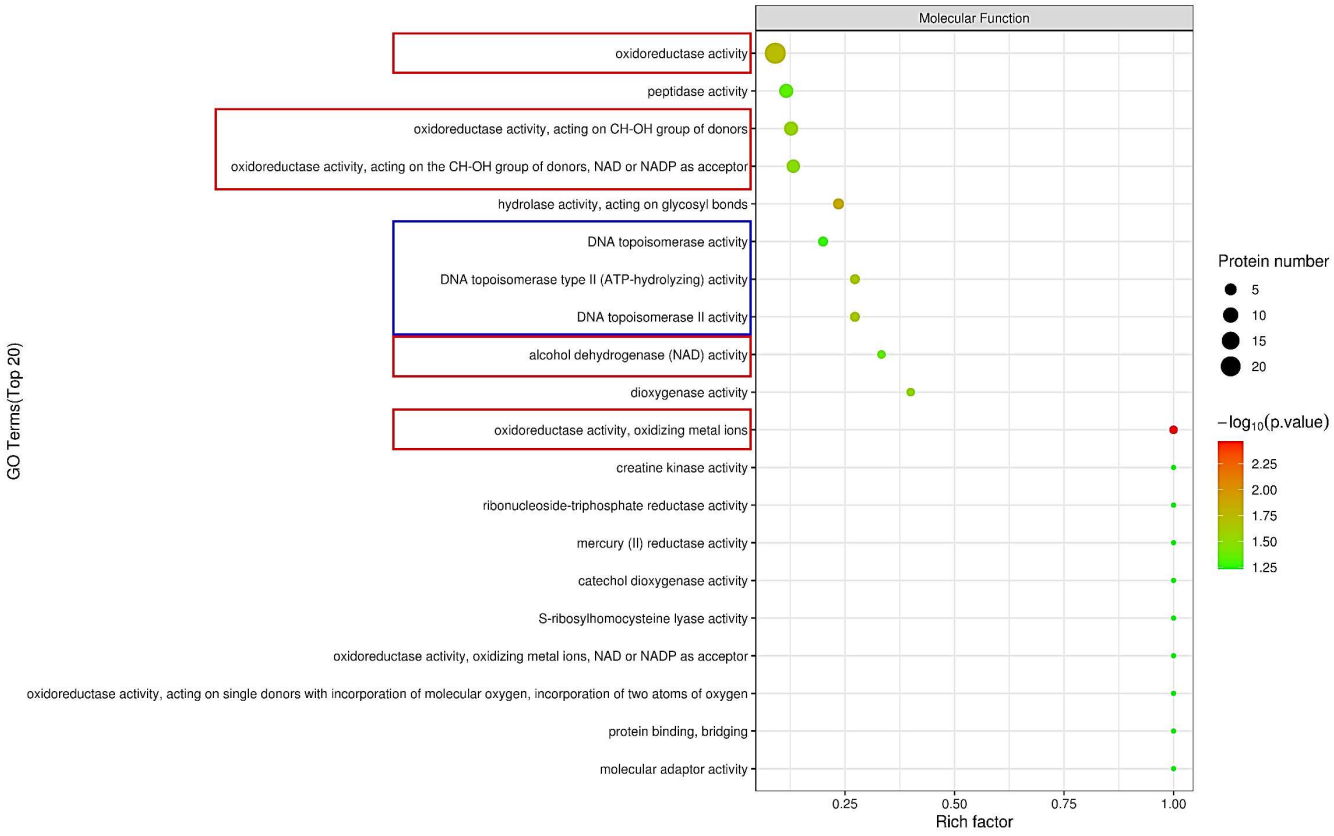

Figure S12. GO function enrichment bubble chart under Molecular Function classification. Enzyme pathways associated with redox and energy metabolism are labeled in red boxes, while enzyme pathways related to DNA function are marked with blue boxes.

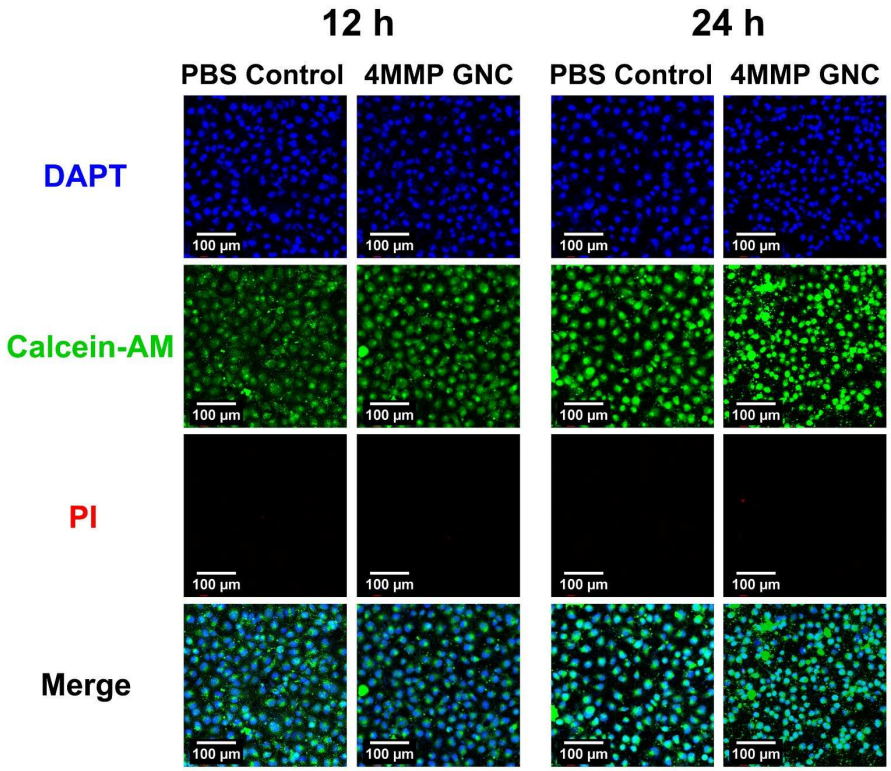

Figure S13. Biocompatibility of 4MMP-GNC towards HUVECs. The cell live-dead staining results of HUVECs after 12 or 24 h incubation with 120 μg mL^{-1} 4MMP-GNC. No increase in cell death (indicated with PI fluorescence) was observed in the 4MMP-GNC-treated group compared with the PBS control.

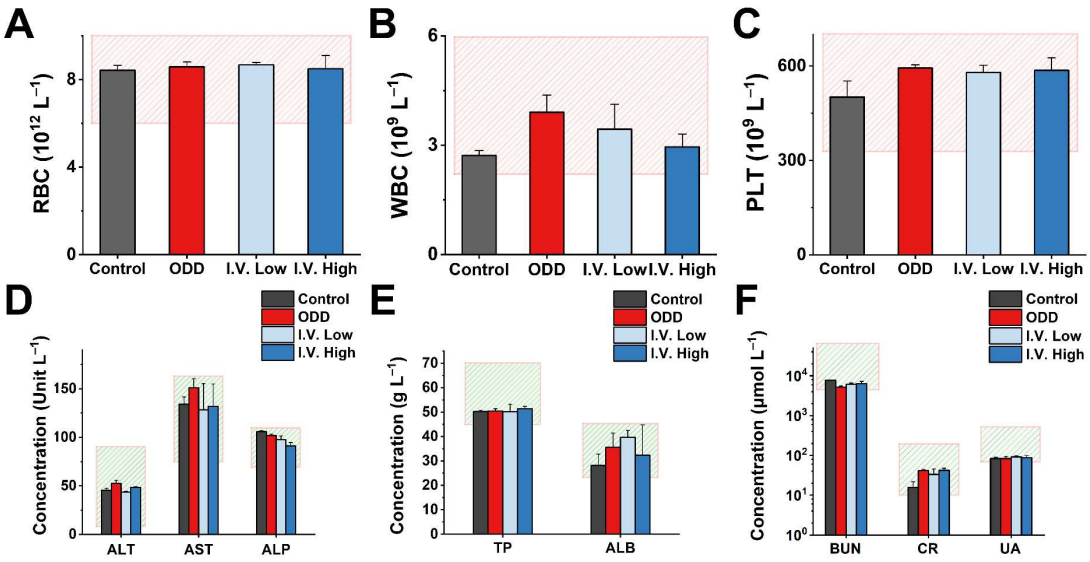

Figure S14. The red blood cell (RBC) (A), white blood cell (WBC) (B), and platelet (PLT) (C) cell number statistics of 4MMP-GNC with ocular drug delivery (ODD) and intravenous administration. (ODD concentration: 120 μg mL^{-1}, low concentration: 6 mg kg^{-1}, high concentration: 12 mg kg^{-1}, same below) Liver function indices: (D) alanine aminotransferase (ALT), aspartate aminotransferase (AST), alkaline phosphatase (ALP), (E) total protein (TP), and albumin (ALB). Kidney function indices: (F) uric acid (UA), creatinine (CR), and blood urea nitrogen (BUN). All the blood indices are within the normal range, indicated with slash boxes (n = 4).

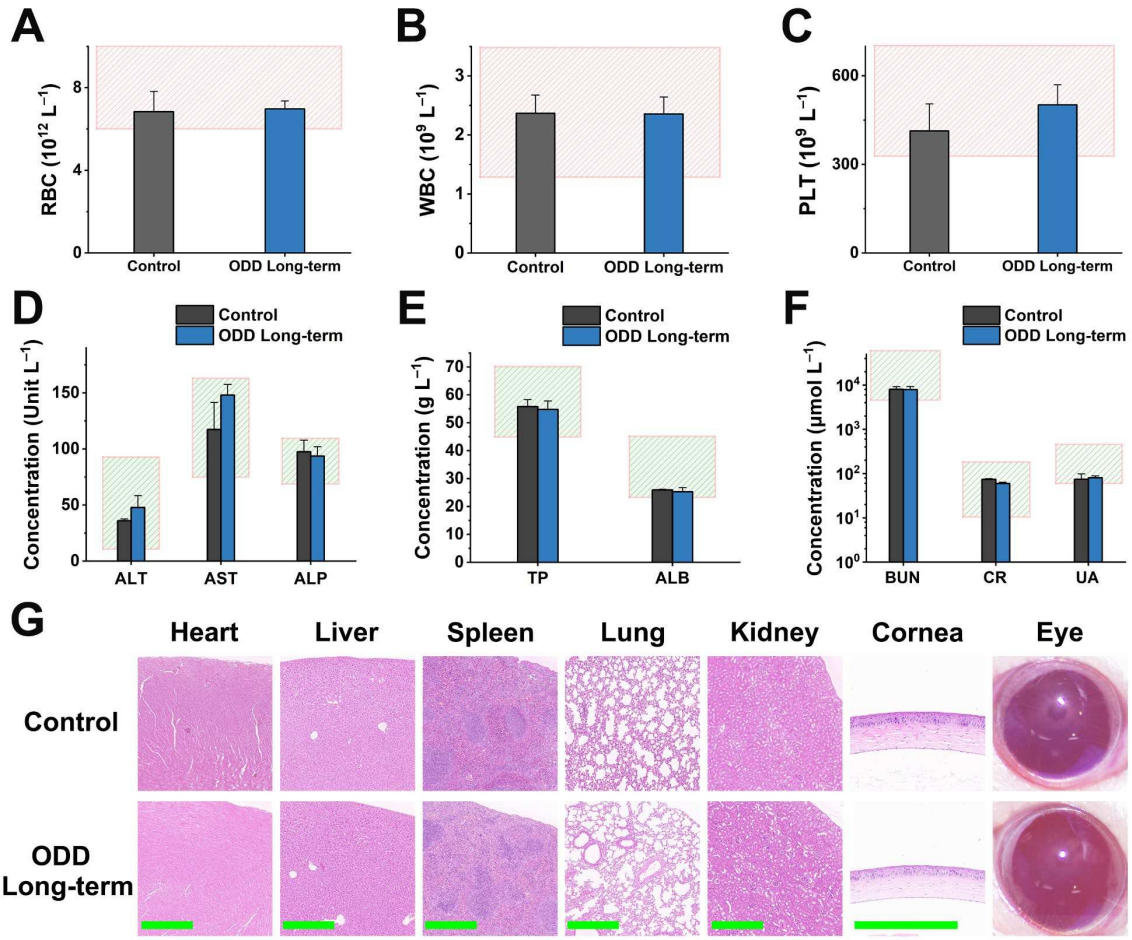

Figure S15. Long-term ODD safety analysis. The RBC (A), WBC (B), and PLT (C) cell number statistics of 4MMP-GNC with 21-day ODD (2 μL, 120 μg mL^{-1}). Liver function indices: (D) ALT, AST, ALP, (E) TP, ALB. Kidney function indices: (F) UA, CR, and BUN. All the blood indices are within the normal range, indicated with slash boxes (n = 4). (G) H&E staining results of the main organs, cornea, and the photographs of eyes after ODD treatment with 4MMP-GNC for 21 days (scale bar: 400 μm).

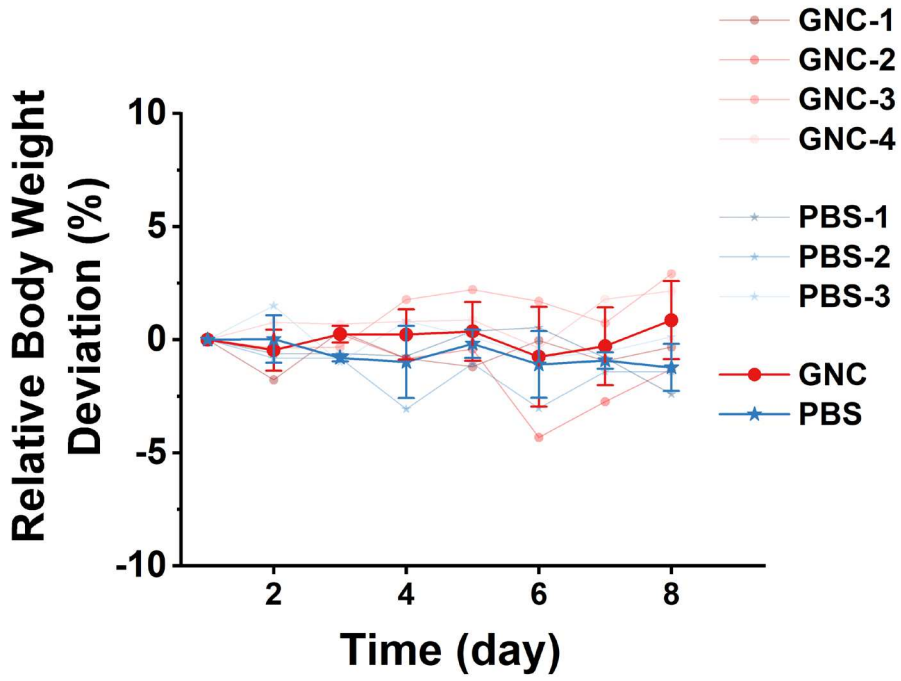

Figure S16. The plot of body weight change of mice challenged with an extremely high concentration of 4MMP-GNCs (110 mg kg^{-1}, 55× MIC). Although exposed to such high concentrations of 4MMP-GNC, there was no mortality in the tested subjects, with their body weights remaining within the normal range compared to the control group. No visible weight loss was observed (n = 4).

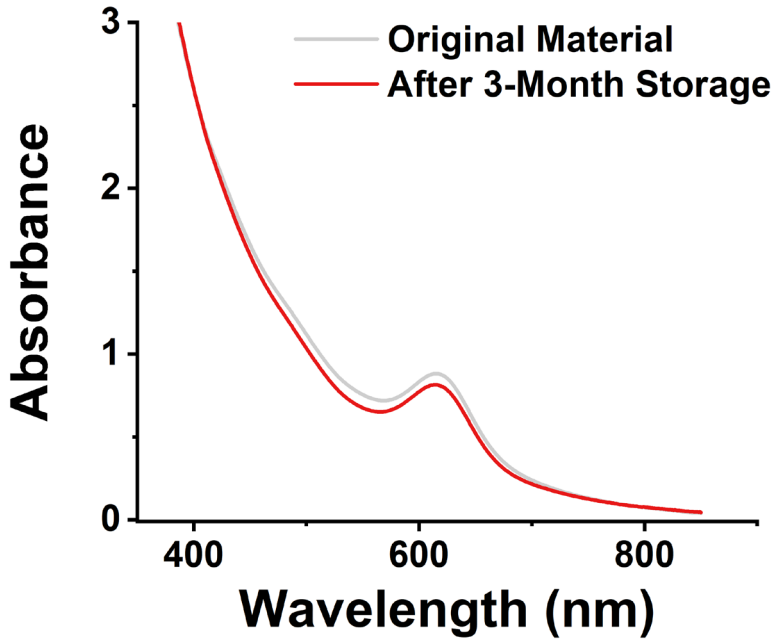

Figure S17. Comparison of UV−vis spectra of the original 4MMP-GNC solution before (grey line) and after storage (red line) for 3 months.

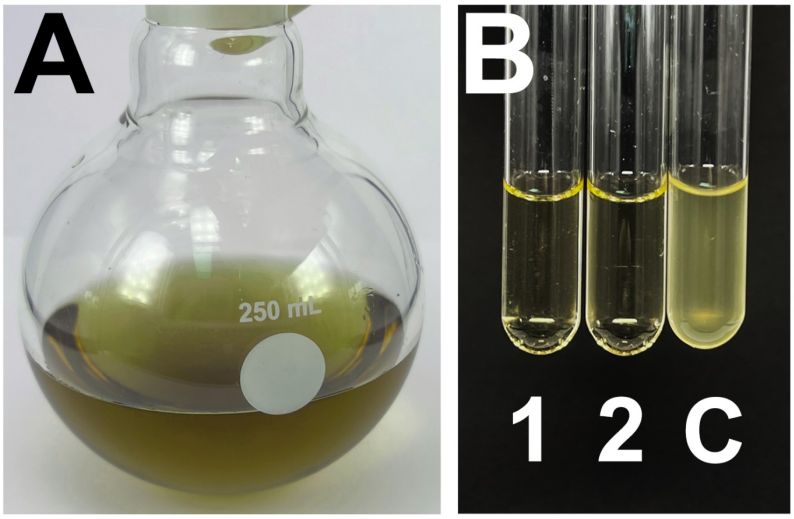

Figure S18. Large-scale preparation of 4MMP-GNC. (A) Optical photo of 4MMP-GNC prepared in a 100 mL scale (20 times the original volume). (B) Comparison of the antibacterial effect of the PBS control (**C**), the scale-up materials (**1,** 2 μg mL^{-1}), and the small-scale preparation materials (**2**, 2 μg mL^{-1}).

3. Reference

[1] Z. Pang, Q. Li, Y. Jia, W. Yan, J. Qi, Y. Guo, F. Hu, D. Zhou, X. Jiang, *Chem. Sci.* **2021**, *12*, 14871.

[2] X. Yuan, B. Zhang, Z. Luo, Q. Yao, D. T. Leong, N. Yan, J. Xie, *Angew. Chem. Int. Ed.* **2014**, *53*, 4623.

[3] C. Wölk, H. Youssef, T. Guttenberg, H. Marbach, G. Vizcay-Barrena, C. Shen, G. Brezesinski, R. D. Harvey, *ChemPhysChem* **2020**, *21*, 702.

[4] M. J. Abraham, T. Murtola, R. Schulz, S. Páll, J. C. Smith, B. Hess, E. Lindahl, *SoftwareX* **2015**, *1–2*, 19.

[5] J. Wang, R. M. Wolf, J. W. Caldwell, P. A. Kollman, D. A. Case, *J. Comput. Chem.* **2004**, *25*, 1157.

[6] A. Das, T. Li, K. Nobusada, C. Zeng, N. L. Rosi, R. Jin, *J. Am. Chem. Soc.* **2013**, *135*, 18264.

[7] E. Pohjolainen, X. Chen, S. Malola, G. Groenhof, H. Häkkinen, *J. Chem. Theory Comput.* **2016**, *12*, 1342.

[8] J. Wang, W. Wang, P. A. Kollman, D. A. Case, *J. Mol. Graph. Model.* **2006**, *25*, 247.

[9] T. Lu, F. Chen, *J. Comput. Chem.* **2012**, *33*, 580.

[10] G. Bussi, D. Donadio, M. Parrinello, *J. Chem. Phys.* **2007**, *126*, 014101.

[11] E. F. Pettersen, T. D. Goddard, C. C. Huang, E. C. Meng, G. S. Couch, T. I. Croll, J. H. Morris, T. E. Ferrin, *Protein Sci.* **2021**, *30*, 70.

[12] L. L. Ling, T. Schneider, A. J. Peoples, A. L. Spoering, I. Engels, B. P. Conlon, A. Mueller, T. F. Schäberle, D. E. Hughes, S. Epstein, M. Jones, L. Lazarides, V. A. Steadman, D. R. Cohen, C. R. Felix, K. A. Fetterman, W. P. Millett, A. G. Nitti, A. M. Zullo, C. Chen, K. Lewis, *Nature* **2015**, *517*, 455.

[13] Y. Xie, Y. Y. Liu, J. Yang, Y. Y. Liu, F. Hu, K. Zhu, X. Jiang, *Angew. Chem. Int. Ed.* **2018**, *57*, 3958.

[14] Y. Xie, J. Yang, J. Zhang, W. Zheng, X. Jiang, *Angew. Chem. Int. Ed.* **2020**, *59*, 23471.

[15] S. Kalita, R. Kandimalla, A. C. Bhowal, J. Kotoky, S. Kundu, *Sci. Rep.* **2018**, *8*, 5778.

[16] S. Wang, Y. Wang, Y. Peng, X. Yang, *ACS Appl. Mater. Inter.* **2019**, *11*, 8461.

[17] J. Liang, H. Xiong, W. Wang, W. Wen, X. Zhang, S. Wang, *Sensor. Actuat. B-Chem.* **2018**, *255*, 2170.

[18] D. Pranantyo, P. Liu, W. Zhong, E. T. Kang, M. B. Chan-Park, *Biomacromolecules* **2019**, *20*, 2922.

[19] Y. A. Prada, F. Guzmán, C. Ortíz, R. Cabanzo, R. Torres, E. Mejía-Ospino, *Protein J.* **2019**, *38*, 506.

[20] Y. Li, J. Zhen, Q. Tian, C. Shen, L. Zhang, K. Yang, L. Shang, *J. Colloid Interf. Sci.* **2020**, *569*, 235.

[21] K. Zheng, M. I. Setyawati, D. T. Leong, J. Xie, *Bioact. Mater.* **2021**, *6*, 941.

[22] K. Zheng, M. I. Setyawati, D. T. Leong, J. Xie, *Nano Res.* **2021**, *14*, 1026.

[23] K. Zheng, M. I. Setyawati, D. T. Leong, J. Xie, *ACS Nano* **2017**, *11*, 6904.

[24] Y. Wang, M. J. Malkmes, C. Jiang, P. Wang, L. Zhu, H. Zhang, Y. Zhang, H. Huang, L. Jiang, *J. Hazard. Mater.* **2021**, *416*, 126236.

[25] Y. Zheng, W. Liu, Z. Qin, Y. Chen, H. Jiang, X. Wang, *Bioconjug. Chem.* **2018**, *29*, 3094.

[26] Y. Xie, Q. Zhang, W. Zheng, X. Jiang, *ACS Appl. Mater. Inter* **2021**, *13*, 35306.

[27] J. Meng, Y. Gao, W. Li, J. Wang, X. Chen, *Talanta* **2021**, *234*, 122618.

[28] F. Gong, R. Peng, Q. Wu, H. Zhang, Y. Luo, Q. Cui, *Colloid. Surface. A* **2022**, *641*, 128608.

[29] P. Zhuang, K. Li, K. Qian, D. Li, X. Mei, *IET Nanobiotechnol.* **2020**, *14*, 412.

[30] Y. Xie, W. Zheng, X. Jiang, *ACS Appl. Mater. Inter.* **2020**, *12*, 9041.

[31] K. Zheng, K. Li, T. Chang, J. Xie, P. Chen, *Adv. Funct. Mater.* **2019**, *29*, 1904603.

[32] Y. Zheng, W. Liu, Y. Chen, C. Li, H. Jiang, X. Wang, *J. Colloid Interf. Sci.* **2019**, *546*, 1.

[33] H. Zhu, J. Li, J. Wang, E. Wang, *ACS Appl. Mater. Inter.* **2019**, *11*, 36831.

[34] K. Zheng, S. Li, L. Jing, P.-Y. Chen, J. Xie, *Adv. Healthc. Mater.* **2020**, *9*, e2001007.

[35] J. Meng, Z. Hu, M. He, J. Wang, X. Chen, *J. Colloid Interf. Sci.* **2021**, *602*, 846.

[36] Y. Zhuo, Y. Zhang, B. Wang, S. Cheng, R. Yuan, S. Liu, M. Zhao, B. Xu, Y. Zhang, X. Wang, *Appl. Mater. Today* **2022**, *27*, 101453.

[37] D. P. Linklater, X. Le Guével, G. Bryant, V. A. Baulin, E. Pereiro, P. G. T. Perera, J. V. Wandiyanto, S. Juodkazis, E. P. Ivanova, *ACS Appl. Mater. Inter.* **2022**, *14*, 32634.

[38] W. Ndugire, N. G. H. Raviranga, J. Lao, O. Ramström, M. Yan, *Adv. Healthc. Mater.* **2022**, *11*, e2101032.

[39] Z. Cao, X. Chen, J. Chen, A. Xia, B. Bacacao, J. Tran, D. Sharma, L. A. Bekale, P. L. Santa Maria, *Nanoscale* **2022**, *14*, 10016.

[40] W. Ndugire, D. Truong, N. G. Hasitha Raviranga, J. Lao, O. Ramström, M. Yan, *Angew. Chem. Int. Ed.* **2023**, *62*, e202214086.

[41] S. Huang, Y. Song, X. Chen, Q. Min, J. Zhang, J. Zhu, *Adv. Funct. Mater.* **2023**, 2300145.